TRIBHUVAN UNIVERSITY

INSTITUTE OF ENGINEERING

PULCHOWK CAMPUS

THESIS NO : S008/075

Form Finding And Optimization Of Grid Shells Using Force Density Method And Discrete Airy Stress Functions

by

Nishan Thapa

A THESIS REPORT

SUBMITTED TO THE DEPARTMENT OF CIVIL ENGINEERING

IN PARTIAL FULFILLMENT OF THE REQUIREMENTS FOR THE

DEGREE OF MASTER IN

STRUCTURAL ENGINEERING

DEPARTMENT OF CIVIL ENGINEERING

LALITPUR, NEPAL

SEPTEMBER, 2021

TRIBHUVAN UNIVERSITY
INSTITUTE OF ENGINEERING
DEPARTMENT OF CIVIL ENGINEERING
PULCHOWK CAMPUS

This is to certify that this thesis work entitled "**Form Finding and Optimization of Grid Shells Using Force Density Method and Discrete Airy Stress Functions**" submitted by Nishan Thapa (075/MSStE/008) has been supervised and recommended to the Institute of Engineering for the partial fulfillment of requirement for the degree of Master of Science in Structural Engineering.

..……
Supervisor, Dr. Bharat Mandal
Department of Civil Engineering
Pulchowk Campus, Institute of Engineering

…….
External Examiner, Dr. Manjip Shakya
Senior Lecturer/ Head of Department
Post Graduate Department of Earthquake Engineering
Khwopa Engineering College

..……
Msc. Co-ordinator, Dr. Kamal Bahadur Thapa
Department of Civil Engineering
Pulchowk Campus, Institute of Engineering

September 2021

COPYRIGHT

ABSTRACT

Force Density Method is widely used method for form finding of tensile cable nets and grid shells. In this thesis, a design tool that utilizes force density method along with Genetic Algorithm have been formulated in Rhino-Grasshopper, a parametric environment, for form finding and optimization of grid shells. Parametric study of a 12m *12m rectangular grid shell for variations in structural weight, height and deflection has been done for various topologies, subdivisions, and force density values. Genetic Algorithm has been used for optimization of grid-shell to get minimum weight for prescribed grid shell heights. Moreover, Force Density Method along with Airy stress functions in discrete form have been utilized for form finding of grid shells of various geometries. Using force density values and grid shell topology the projection of discrete airy stress function in form of plane faced polyhedron, form finding of grid shell self-supporting in lateral direction has been done. Variations in structural parameters between grid shell forms obtained using stress polyhedron and forms obtained using uniform force densities have been studied.

ACKNOWLEDGEMENT

I wish to express my sincere gratitude to my supervisor Dr. Bharat Mandal, for his continuous guidance, inspiration and encouragement during the thesis work and study period. His lectures and advice proved to be valuable in process of this thesis work.

I would also like to acknowledge all the faculty members of Department of Civil Engineering for the knowledge and concepts they gave me during my study at IOE, Pulchowk Campus.

I would like to express my very great appreciation to Er. Pramod Tiwari, Er. Prabin Wagle, Er. Bijay Ban, Er. Pradeep Tamang and my classmates for their direct and indirect help over the period of master's study as well as this thesis.

To my family, thank you for encouraging me in all my dreams and inspiring me during the thesis work.

I would like to recognize the assistance obtained through the reference books and research papers and would like to thank their authors.

Nishan Thapa

075/MSStE/008

September 2021

TABLE OF CONTENTS

COPYRIGHT 3

ABSTRACT 4

ACKNOWLEDGEMENT 5

LIST OF FIGURES 8

LIST OF TABLES 11

CHAPTER 1: INTRODUCTION 13

1.1 Introduction 13
1.2 Problem Statement/Motivation 16
1.3 Purpose and Objectives of the study 16
1.4 Limitations of the study 16
1.5 Thesis Organization 17

CHAPTER 2: LITERATURE REVIEW 18

2.1 General 18
2.2 Graphic Statics 18
2.3 Reciprocal Diagrams and Airy Stress Functions 18
2.4 Force Density Method or Analysis methods 19

CHAPTER 3: METHODOLOGY 21

3.1 Formulation of Force Density Method (FDM) 21
3.2 Validation of FDM formulation 26
3.3 Structural weight and total load path 28
3.4 Force density 29
3.5 Grid shell loading 29
3.6 Airy Stress Function and form polyhedron 32
3.7 Airy Stress formulation for grid shells 33
3.8 Genetic Algorithm 36

CHAPTER 4: RESULTS AND DISCUSSIONS 38

4.1 Form finding shells with irregular boundary shapes 38
4.2 Parametric variation in weight, height and deflection using FDM 40
4.2 Optimization for weight and height 45
4.3 Discrete Airy stress function and FDM 46
4.3.1 Rectangular plan grid shell 46

4.3.2 Circular plan grid shell 50
4.3.3 Structures obtained by variation of support condition 53
CHAPTER 5: CONCLUSION 55
5.1 Conclusions 55
5.2 Further recommendations 55
REFERENCES 56
ANNEX I 59
ANNEX II 62

LIST OF FIGURES

Figure 1 Continuous Shell - L'Oceanografic, City of Arts and Sciences, (L'Oceanografic, n.d.) 13

Figure 2 Grid Shell - Glass roof Dutch Maritime Museum (Glass roof Dutch Maritime Museum at Amsterdam, Netherlands, n.d.) 13

Figure 3 (a) A simple grid system. Nodes are denoted by plain numbers. Branches are denoted by circled numbers; (b) The connectivity matrix of the grid system (Jiang, 2015) 23

Figure 4 Force Density Method workflow 25

Figure 5 2D Bar network - input of FDM 26

Figure 6 Form found grid shell with FDM 27

Figure 7 ETABS model of the grid shell 27

Figure 8 Plan view of grid shell with member labeling 27

Figure 9 Loading error for quadrangular grid shell for various force density and 6 subdivisions 30

Figure 10 Loading error vs no. of iterations for various grid shell topologies at force density 20KN/m and 6 subdivisions. 30

Figure 11 Flow Chart of Methodology for grid shell design and optimization using FDM. 31

Figure 12 Flow Chart of Methodology for grid shell design and optimization using . 31

Figure 13 Continuous Airy Stress Function over continuous surface (Baker, 2021) .. 33

Figure 14 Discrete Airy Stress Function at intersection of two planes (Baker, 2021) 33

Figure 15 General overview of Evolutionary solver mechanism (Cheng, 2018) 36

Figure 16 Basic Workflow for grid shell design using FDM only and FDM with Airy Stress Function. 37

Figure 17 Grid shell typologies considered in study. 40

Figure 18 Variation of grid shell height as per grid density for force density of 25KN/m. 41

Figure 19 Variation of grid shell structural weight as per grid density for force density of 25KN/m. 42

Figure 20 Variation of grid shell deflection with numbers of subdivision for force density of 25 KN/m. 42

Figure 21 Variation of grid shell height as per force density for 12 subdivisions. 43

Figure 22 Variation of grid shell structural weight as per force density for 12 subdivisions 44

Figure 23 Variation of grid shell structural weight as per force density for 12 subdivisions 44

Figure 24 Grid shell form obtained for minimum structural weight as per case 1. 46

Figure 25 Grid shell form obtained for grid shell height of 1.5m as per case 2. 46

Figure 26 Grid shell plan with supports and member connectivity 48

Figure 27 Plan view of Grid shell after form-finding with FDM (FD = 15 KN/m) 48

Figure 28 Perspective view of Grid shell after form-finding with FDM (FD = 15 KN/m) 48

Figure 29 Perspective view of Grid shell support reaction (Reaction units in KN) 48

Figure 30 Plan view of Grid shell after form-finding with force density values input from Airy Stress Function taken to be grid shell form at Figure 31 49

Figure 31 Perspective view Grid shell after form-finding with force density values input from Airy Stress Function taken to be grid shell form at Figure 31 49

Figure 32 Perspective view Grid shell and support reactions after form-finding with force density values input from Airy Stress Function taken to be grid shell form at Figure 31 49

Figure 33 Plan view of stress polyhedron for circular type grid shell 51

Figure 34 Projection of stress polyhedron of circular type grid shell representing base geometry for FDM 51

Figure 35 3D view of stress polyhedron for circular type grid shell 51

Figure 36 Plan view of grid shell geometry obtained from FDM using uniform force density. 52

Figure 37 3D view of grid shell geometry obtained from FDM using uniform force density. 52

Figure 38 Plan view of grid shell geometry obtained from FDM using force density values from stress polyhedron. 52

Figure 39 3D view of grid shell geometry obtained from FDM using force density values from stress polyhedron. 52

Figure 40 Grid shell geometry formed lofting edges to circular arc..... 63

Figure 41 Grid shell constructed with pyramidal geometry 63

Figure 42 Form found grid shell 63

LIST OF TABLES

Table 1 Literature review with respective methodology 20

Table 2 Parameters for FDM and FEM 26

Table 3 Variation in member forces between FDM and ETABS.....28

Table 4 Reciprocity of Airy Stress Function and Grid shell geometry.....35

Table 5 Variations of grid shell geometries obtained for boundary (red line) and support (red dot) for various grid densities, force densities and topologies. 39

Table 6 Grid shell height, weight and deflection variation for variation in topology for 8 no. of divisions and force density 25KN/m. 40

Table 7 GA Optimization result for structural weight and height 45

Table 8 Comparison of basic parameters using FDM and FDM along with stress polyhedron for rectangular plan grid shell.....50

Table 9 Comparison of basic parameters using FDM and FDM along with stress polyhedron for circular plan grid shell.....53

Table 10 Various shapes generated from Airy Stress Function.....54

Table 11 Deflection and mass comparison table for lateral load in grid shells. 62

Table 12 Lateral load effects on various grid shell geometries 63

LIST OF SYMBOLS

σ_{xx}	Normal stress along x-axis
σ_{yy}	Normal stress along y-direction
τ_{xy}	Shear stress in XY plane
φ	Airy stress function
N_n	No. of modes
N_b	No. of branches/members
N_f	No. of fixed nodes
N	No. of free nodes
Cs	Branch Node Connectivity Matrix
C	Branch Node Connectivity Matrix for free nodes
C_f	Branch Node Connectivity Matrix for fixed nodes
q	Force density of a member
Q	Force density matrix
U	Co-ordinate Difference Matrix along x direction
V	Co-ordinate Difference Matrix along y direction
W	Co-ordinate Difference Matrix along z direction
p_x	Nodal load along x-direction
p_y	Nodal load along y-direction
p_z	Nodal load along z-direction
s	Member force
L	Member length
$X_{f,}$	Fixed node coordinate vector along x-direction
Y_f	Fixed node coordinate vector along y-direction
Z_f	Fixed node coordinate vector along z-direction
X	Free node coordinate vector along x-direction
Y	Free node coordinate vector along y-direction
Z	Free node coordinate vector along z-direction

CHAPTER 1: INTRODUCTION

1.1 Introduction

A structure in which the thickness is small compared to other dimensions is generally called a thin shell. Thin shells are often the priority choice for long span roofing structures throughout the world for their aesthetic beauty and efficient transfer of loads with low structural weights, deriving strength from their form and geometry. Generally, thin shells can be categorized into two branches, namely, 1. continuous shells -as the name suggests are composed of continuous shell surface throughout the area of load transfer and 2. Grid-shells: composed of discrete grid members as structural elements, often steel or timber. Images of some famous grid-shell and continuous shells are shown in Figure 1 and Figure 2. The thesis is focused on grid-shells.

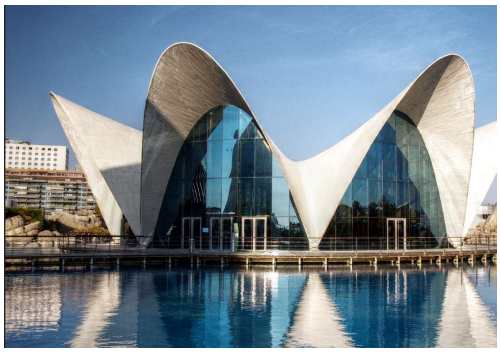

Figure 1 Continuous Shell - L'Oceanografic, City of Arts and Sciences, *(L'Oceanografic, 2021)*

Figure 2 Grid Shell - Glass roof Dutch Maritime Museum *(Glass roof Dutch Maritime Museum at Amsterdam, Netherlands, 2017)*

In design of shell structures, the form and structural efficiency cannot be separated as the form regulates force flow and choice of a structurally efficient form can be realized in various forms. Shell geometry largely determine the characteristics and magnitude of forces arising in the members. The design of these structures in the usual workflow follows form design by architect, then structural design by structural engineer and construction by craftsmen. A major drawback of this workflow, in most cases, is that the structures are often uneconomical and sometimes unfeasible to construct, because of the fixed geometrical domain within which structural designers and craftsmen must work with. This drawback can be minimized by incorporating the basic structural and buildability constraints during initial design phase of the project. A well-conceived

geometry and topology of structures can obviate a lot of design hurdles and reduce the project costs considerably. Here a convenient tool is proposed for the form finding of grid-shells, in a parametric environment (Rhino-grasshopper), addressing the structural requirements.

Shell geometries for design can be distinguished mainly in three types, namely Freeform shells where shapes are taken arbitrarily, Mathematical shells taken for their convenience in fabrication and analytical calculations and Form-found shells, mainly natural hanging shapes associated with funicular structures (Adriaenssens, Block, Veenendaal, & Williams, 2014). Form finding is a forward process in which parameters are explicitly/directly controlled to find an 'optimal' geometry of a structure which is in static equilibrium with a design loading (Adriaenssens, Block, Veenendaal, & Williams, 2014). In general, form found shells are structurally robust and optimized for design requirements, when compared to other shell geometries.

For shells, methods like Dynamic relaxation methods, hanging chain models, Force density methods are often used for funicular form finding where every member is either in compression or in tension. The major limitation of these methods is that, on their own they can only determine the compression or tension only forms, although structurally efficient. Finite Element Methods such as stiffness matrix methods, considering both tension-and-compression members, are often applied at later stages of design for verifications because of their higher computational demand during early stages of form finding (Veenendaal & Block, 2012). Also, modelling a fully formed 3D form is cumbersome often inviting various errors.

The force density method was developed by Schek (1974) for finding equilibrium state of given pin-joint network consisting of cables or bars subjected to pre-stressing or any external loading with low computation costs. Preassigning force density, which is the force in member divided by its length, linearizes the geometrically non-linear equilibrium problem, thus finding the equilibrium shape in a direct way.

Force density variation with systematic manual input or assignment through results of plane faced airy stress polyhedron as in (Konstantatou, 2019) as well as assignments of various geometrical and boundary constraints can be done to obtain various funicular shapes, also tension and compression structures. A 2D self-stressed pinned structure in equilibrium, can be created from projection of a closed plane faced polyhedron,

equivalent to 3D Airy stress Function, with member forces of the structure equal to the change in curvatures of two planes in Airy stress polyhedron, whose intersection form the member. Thus, these form finding methods mainly Force Density Method could be used in conjunction with Airy Stress Function to solve the general case of tension- and-compression grid-shells (Konstantatou, 2019).

Starting design from plane polyhedral Airy Stress Function ensures the equilibrium of structure which can be modified as per buildability and site-specific boundary constraints to determine the optimum form of grid shells. Furthermore, the structure is self-supporting i.e., reducing the lateral loads in the support, which could be extremely helpful when grid shells are to be constructed in conjunction with prebuilt or historic structures.

In this study, we employ Force Density Method (FDM), a method of form-finding, FEM for deflection and various load case analysis and genetic algorithm (GA) for design and optimization of grid-shells. Further, Discrete Airy Stress Function (DASF) in form of plane faced polyhedron is used in conjunction of FDM for form finding and rest of the process following the same as before. Here, a design tool is developed in widely used software- Rhino, that assist architects and engineers at early stages of design from form finding as well as discretization and optimization of grid shell, that would prove to be beneficial, minimizing the structural costs while satisfying architectural and structural demands.

Case studies of a 12m x 12m rectangular grid shell is done varying mainly parameters like force density, grid density and grid shapes regarding its effect on the structural height, structural weight, and deflection. Optimization is done for the same shell using GA to determine shell configuration with minimum weight regardless of consideration for height and separately for shell to have a height equal to 1.5m. For the shell of same geometry but varying topology, Discrete Airy stress function in the form of plane faced polyhedron, henceforth referred as stress polyhedron, is used to determine force density input values to determine self-stressed grid shell structures. The results are compared with the case of grid shell obtained using FDM alone. Further, various self-supporting structures (in lateral direction) obtained using FDM and stress polyhedron are explored.

1.2 Problem Statement/Motivation

Although, having high efficiency in load transfer for their low self-weight and structural integrity, because of fabrication difficulties and computational hurdles, grid-shells are often disregarded in developing countries as Nepal. Geometrical methods of structural analysis and design of trusses and grid-shells not only allows for intuitive understanding of how loads are transferred within the structure, but it also simplifies the optimization ensuring the structural integrity. Thus, Geometrical methods are proposed for exploration to determine efficient structures for load transfers mainly in case of long span roofing using Discrete Airy Stress functions.

1.3 Purpose and Objectives of the study

The general objective of this research is to explore the Form Finding and Optimization of grid-shells.

The specific objectives include:

- Determine the variation of grid shell weight, height, and deflection values for variation in grid density (shape), topology and force density values in a case study of a 12m*12m rectangular grid shell.
- Determine optimum grid shell for given limitations in weight, height, and deflection values.
- Study variations among grid shells determined using uniform force density and force densities from stress polyhedron.
- Develop a design tool that suggests structurally robust grid-shell forms at early phase of design.

1.4 Limitations of the study

The limitations of the study are listed below:

- Uniform static gravity load over shell surface is taken as dominant load case and transferred to nodes as per tributary area.
- Consideration for buckling and global stability has not been done.
- Connections are assumed to be hinged and connection complexities are not taken as parameters in optimization.

1.5 Thesis Organization

The remainder of the thesis is organized as follows. The literature review on major concepts is presented in chapter 2 with some historical backgrounds. The methodology is presented in Chapter 3, which outline the formulation of force density method, demonstrates the fundamentals of Airy Stress Function and its representation of Reciprocal polyhedral in graphic statics, and optimization algorithm. The details of work procedure will also be presented in Chapter 3. In Chapter 4, results, and discussions of case study of a rectangular plan grid shell form finding and design optimization as well will be presented, as well as the ability of design tool formulated. Chapter 5 presents the conclusions and further recommendations of the thesis.

CHAPTER 2: LITERATURE REVIEW

2.1 General

Many research articles related to approaches for structural optimization and form finding of grid-shells are studied. Most notable ones are as follows:

2.2 Graphic Statics

Considerable work has been done in graphical analysis of trusses by Maxwell J. (1864) and Maxwell J. (1870) which expresses the reciprocity between form and force diagrams. Although being used throughout the 20th century though scarcely, over the last few decades, graphic statics has seen renewed interest. Recent applications of graphic statics are underpinned by the computational and visual capabilities offered by contemporary computer aided design tools. These can be found among others in the design of compression-only or tension only spatial funicular structures by means of the Thrust Network Analysis (TNA) (Block & Ochsendorf, 2007), which combines 2D graphic statics with the force density method. Beghini et al. (2014) reestablish graphic statics as a structural optimization tool of discrete trusses exploring advantages of this method over conventional methods of analysis, design, and optimization.

2.3 Reciprocal Diagrams and Airy Stress Functions

In 2D reciprocal diagrams, form edges map to force edges and form nodes to closed force polygons, obeying 3D duality. These reciprocal diagrams are projections of polyhedral Airy Stress functions which are reciprocal as well. Maxwell J. (1870) said that this reciprocity between polyhedral can be obtained through a polar transformation, using paraboloid of revolution. The change of slope between adjacent faces of the Airy Stress function defines the axial force of the corresponding structural member of the 2D truss (McRobie, Baker, Mitchell, & Konstantatou, 2016) (Mitchell, Baker, McRobie, & Mazurek, 2016). Moreover, the roles of reciprocal form and force diagrams are interchangeable an there are no distinctions between lines of action of the applied forces and structural members as the internal or external forces can be combined with the form diagram to make projection of a single polyhedron truss (McRobie, Baker, Mitchell, & Konstantatou, 2016) (Mitchell, Baker, McRobie, & Mazurek, 2016). Thus, this polyhedron can be seen as the Airy Stress function of an equivalent self-stressed truss. Further, Miki et al.(2020) investigated tension-compression mixed type shells by

utilizing a NURBS-based iso-geometric form-finding approach that use Airy stress functions to expand the possible plan geometry.

2.4 Force Density Method or Analysis methods

The fundamental rationale of the 3D hanging chain model has long been discussed, as a quotation from Robert Hooke in 1675 says "As hangs a flexible cable, so but inverted will stand the rigid arch." This principle describes the reciprocal relationship of a tension-only and a compression-only form in 2-dimensional (2D) space under the same loading case (Block & Ochsendorf, 2007). When extended to design in the 3-dimensional (3D) space, this rationale supports the use of the 3D hanging chain model for the form finding of a gravity-loaded structure (Jiang, 2015).

The force density method (Schek, 1974) or 'Stuttgart direct approach' was primarily used for form-finding and design explorations of prestressed spatial tension-only structures, such as hanging cable nets and membranes (Adriaenssens, Block, Veenendaal, & Williams, 2014). For this type of funicular structures, the form is interlinked to the internal forces and greatly affects the load-bearing behavior (Adriaenssens, Block, Veenendaal, & Williams, 2014).

Extension the potential and robustness of FDM has been done in form-finding of compression and tension structures such as tensegrities and suspended bars (Miki & Kawaguchi, 2010). The Discrete polyhedral stress function has been introduced (Fraternali, 2010) for the analysis of unreinforced masonry vaults and for the prediction of fracture-prone regions. Further, various studies for evaluation of grid shell performance and structural weight varying similar parameters have been done by various researchers, to name few, (Malek, 2012) using FEM for analysis, (Olsson, 2012) using SMART form, (Green & Lauri, 2017) using Dynamic relaxation. Konstantatou (2019) combines the Discrete Airy Stress Function with Force density method as design exploration for grid shells containing both compression and tension.

Most of the research work are focused on implementing and extending the design and optimization of funicular form shells/grid-shells with very few focusing on both tension-compression grid-shells. Moreover, only a few research have been done combining the Discrete Airy Stress Method with Form finding method as FDM, although, leaving room for extended parametric study and application of this combination for design exploration. Thus, as an extension to the earlier works, it is

proposed to combine Airy stress function method with FDM along with optimization methods to explore a robust design space.

Some literature reviews with their respective methodologies are presented in Table *1*:

Table 1 Literature review with respective methodology

Literature Review	Methodology
(Maxwell J. , 1864) (Maxwell J. , 1870)	Introduces Graphic Statics Method, Shows relation between 3d polyhedral Airy Stress Function and 2d trusses.
(Block & Ochsendorf, 2007)	Combination of 2d Graphic Statics with force density method for compression only or tension only spatial funicular structure.
(Beghini et al., 2014)	Graphic Statics as analysis design and optimization of discrete 2D truss in modern context.
(Miki et al., 2020)	Utilize NURBS based Iso-geometric analysis and Form finding approach using Airy Stress Functions
(Schek, 1974)	Introduction of FDM
(Jiang, 2015)	Compares Potential Energy Method - Dynamic Relaxation and FDM
(Adriaenssens, Block, Veenendaal, & Williams, 2014)	Form-finding and design exploration of pre-stressed spatial tension-only structures
(Konstantatou, 2019)	Combine Airy Stress Function and Force Density Method for design exploration of Grid Shells.
(Airy, 1862)	Introduce Airy Stress Function to calculate strains in frames.

CHAPTER 3: METHODOLOGY

A method for structurally efficient form finding and optimization for grid-shells has been proposed. The visualization as well as computation are done in Rhino – Grasshopper Environment with additional use of Python programming language. Rhino- Grasshopper allows parametric workflow thus facilitating the study of variations of each parameter involved in the study.

FDM formulation has been done in Rhino using Grasshopper and Python for calculation and solving linear equations, while Galapagos plugin within grasshopper has been used for optimization by genetic algorithm. Karamba3D within Grasshopper has been used as a FEM analysis tool for further analysis and to determine deflection.

The initial design settings comprise of grid members, hinge nodes and nodal boundary conditions. Shell panels are considered for nodal load calculation, but not as structural members in the design. As loads are applied, the grid shell form will change so that an equilibrium state is achieved. The design goal is to find a grid form in equilibrium under a certain load case, where the members suffer no bending moment and no shear force. The state of zero bending moment and shear force is ensured by the assumptions that:

1. All grid members are hinge-connected.

2. For every grid member, loads are only applied at the end nodes.

Thus, the task left is to find the equilibrium form.

For the study, buckling has not been considered, connections are assumed to be pin jointed, connection costs been not taken for optimization and only statically uniformly distributed gravity load case has been done. However, Comparison of grid-shells of various geometries (spherical type, pyramidal and form found using FDM) is done for lateral load case, namely, static lateral wind loading in single direction. The comparison clearly shows the superiority of form found grid-shells over other types taken in the comparison. The results are presented in Table 11 and Table 12 in the Annex II.

3.1 Formulation of Force Density Method (FDM)

The force density method or ‘Stuttgart direct approach’ was initially used for form-finding and design explorations of general networks of hanging cables, bars and membranes. The name is derived from ‘Force Density’, a parameter used, that

represents the ratio of member forces by member length. Pre-assigning the Force density linearizes the non-linear geometry and static -equilibrium problem and its solution represent the final form.

The input of the FDM is 2D ground structure with force densities provided for each member and a list of fixed nodes. The output is co-ordinates (x, y and z) of each point in the ground structure. Changing the force density to positive or negative enables one to get a form with members in either tension or compression. Furthermore, fixed member lengths could also be assigned adding to more realistic design.

FDM offers features like (1) Manages equilibrium equations in totally direct way and is therefore especially suited for a funicular solution. (2) Equilibrium equations are linearized, which simplifies the numerical process (3) No member pre-sizing is required (4) The three equilibrium equations are uncoupled (Cercadillo-García & Fernández-Cabo, 2016).

The formulation of FDM is below with major reference to (Schek, 1974) and (Jiang, 2015).

To begin with, we define a grid system with nodes from 1 to Nn and grid members (or branches) from 1 to N_b. To simplify, the calculation process, we define all the fixed nodes (N_f nodes, from N+1 to N+N_f) after all the free nodes (N nodes from 1 to N). Thus, we have $N_n = N+N_f$. For any grid member j, there are 2 corresponding nodes with number c(j) and d(j). With the information above, the branch-node matrix $\mathbf{C}s$ is defined as shown in Equation 3.1.1.

$$\mathbf{C}s(j,i)= \begin{cases} +1, \text{ for } c(j)=i \\ -1, \text{ for } d(j)=i \\ 0, \text{ otherwise} \end{cases} \qquad (3.1.1)$$

The matrix $\mathbf{C}_s$ has N_b rows and N_n columns. Note that the value of c(j) and d(j) for a grid member may interchange with each other. This interchange will affect $\mathbf{C}_s$ but will not influence the resultant linear system.

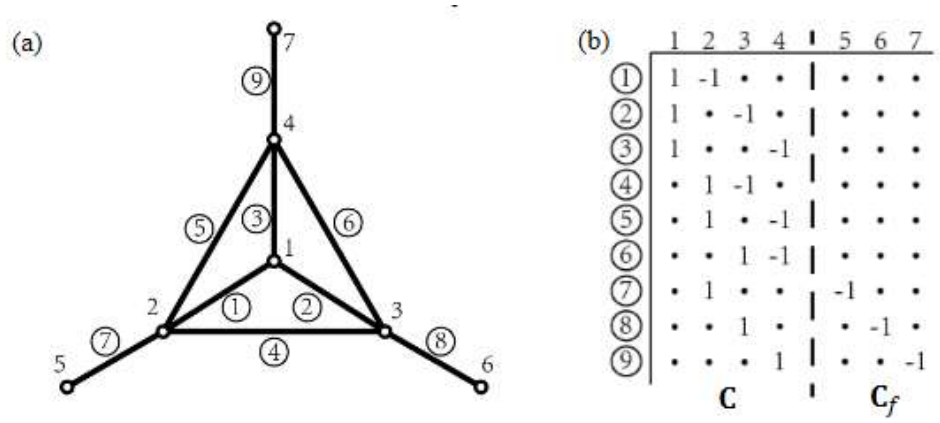

Figure 3 (a) A simple grid system. Nodes are denoted by plain numbers. Branches are denoted by circled numbers; (b) The connectivity matrix of the grid system *(Jiang, 2015)*

The branch-node matrix $\mathbf{C}_s$ is separated into $\mathbf{C}$ and $\mathbf{C}_f$, with $\mathbf{C}$ representing the portion for free nodes and $\mathbf{C}_f$ for the fixed nodes, as illustrated by Figure 3. In a similar logic, $\mathbf{X}$, $\mathbf{Y}$, $\mathbf{Z}$ and $\mathbf{X}_f$, $\mathbf{Y}_f$, $\mathbf{Z}_f$ correspond to the nodal coordinate vectors of free and fixed nodes in the x, y and z directions, respectively. Vectors holding the coordinate difference between 2 connected nodes are defined as u, v, and w. They are derived with branch-node matrices and nodal coordinates, given by equation 3.1.2.

$$\begin{aligned} \mathbf{u}&=\mathbf{C}*\mathbf{X}+\mathbf{C}_f\mathbf{X}_f \\ \mathbf{v}&=\mathbf{C}*\mathbf{Y}+\mathbf{C}_f\mathbf{Y}_f \\ \mathbf{w}&=\mathbf{C}*\mathbf{Z}+\mathbf{C}_f\mathbf{Z}_f \end{aligned} \qquad (3.1.2)$$

Let us define the member length vector as ℓ and the force density vector as q. The force density of the j^{th} grid members q_j is defined as its force-length ratios. Then define U, V, W, L, Q as the diagonal matrices of the vector u, v, w, $\boldsymbol{\ell}$ and q, respectively. Moreover, define s as the member internal force vector. To maintain force equilibrium at every node, the sum of internal forces should equal the external forces.

The equilibrium equations are formulated as shown in Equation 3.1.3.

$$\begin{aligned} \mathbf{C}^{\mathrm{T}}\mathbf{U}\mathbf{L}^{-1}\mathbf{s}&=\mathbf{p}_x, \\ \mathbf{C}^{\mathrm{T}}\mathbf{V}\mathbf{L}^{-1}\mathbf{s}&=\mathbf{p}_y, \\ \mathbf{C}^{\mathrm{T}}\mathbf{W}\mathbf{L}^{-1}\mathbf{s}&=\mathbf{p}_z \end{aligned} \qquad (3.1.3)$$

In the equilibrium equations, representations of Jacobian matrices are utilized, given by equation 3.1.4.

$$\frac{\partial \mathrm{l}}{\partial \mathrm{x}} = \mathbf{C^T U L^{-1}}$$
$$\frac{\partial \mathrm{l}}{\partial \mathrm{y}} = \mathbf{C^T V L^{-1}} \qquad (3.1.4)$$
$$\frac{\partial \mathrm{l}}{\partial \mathrm{z}} = \mathbf{C^T W L^{-1}}$$

The force density vector $\mathbf{q}$ is obtained by:

$$\mathbf{q}=\mathbf{L}^{-1}\,\mathbf{s} \qquad (3.1.5)$$

Where, $\mathbf{L}$ is the diagonal matrix of the member length vector $\boldsymbol{\ell}$, and $\mathbf{s}$ is the member force vector. With (3.1.5), we can then update (3.1.3) into:

$$\mathbf{C}^{\mathrm{T}}\mathbf{U}\mathbf{q}=\mathbf{p}_x$$
$$\mathbf{C}^{\mathrm{T}}\mathbf{V}\mathbf{q}=\mathbf{p}_y \qquad (3.1.6)$$
$$\mathbf{C}^{\mathrm{T}}\mathbf{W}\mathbf{q}=\mathbf{p}_z$$

By means of equation 3.1.2 and equation 3.1.6, we obtain equation 3.1.7 as:

$$\mathbf{U}\mathbf{q}=\mathbf{Q}\mathbf{u}$$
$$\mathbf{V}\mathbf{q}=\mathbf{Q}\mathbf{v} \qquad (3.1.7)$$
$$\mathbf{W}\mathbf{q}=\mathbf{Q}\mathbf{w}$$

The nodal force equilibrium equation systems in x, y and z directions are formulated as equation 3.1.8.

$$\mathbf{C}^{\mathrm{T}}\mathbf{Q}\mathbf{C}\mathbf{x}+\mathbf{C}^{\mathrm{T}}\mathbf{Q}\mathbf{C}_f\mathbf{x}_f=\mathbf{p}_x$$
$$\mathbf{C}^{\mathrm{T}}\mathbf{Q}\mathbf{C}\mathbf{y}+\mathbf{C}^{\mathrm{T}}\mathbf{Q}\mathbf{C}_f\mathbf{y}_f=\mathbf{p}_y \qquad (3.1.8)$$
$$\mathbf{C}^{\mathrm{T}}\mathbf{Q}\mathbf{C}\mathbf{z}+\mathbf{C}^{\mathrm{T}}\mathbf{Q}\mathbf{C}_f\mathbf{z}_f=\mathbf{p}z$$

For a simpler representation, we can write $\mathbf{D}=\mathbf{C}^{\mathrm{T}}\mathbf{Q}\mathbf{C}$ and $\mathbf{D}_f=\mathbf{C}^{\mathrm{T}}\mathbf{Q}\mathbf{C}_f$, so that equation 3.1.8 becomes equation 3.1.9.

$$\mathbf{D}\mathbf{X}+\mathbf{D}_f\mathbf{X}_f=\mathbf{p}_x$$
$$\mathbf{D}\mathbf{Y}+\mathbf{D}_f\mathbf{Y}_f=\mathbf{p}_y \qquad (3.1.9)$$
$$\mathbf{D}\mathbf{Z}+\mathbf{D}_f\mathbf{Z}_f=\mathbf{p}_z$$

Simplifying we get equation 3.1.10, shown as:

$$\mathbf{X} = \mathbf{D}^{-1}\,(\mathbf{p}_x \;-\; \mathbf{D}_f\,\mathbf{X}_f)$$

$$\mathbf{Y} = \mathbf{D}^{-1} (\mathbf{p}_y - \mathbf{D}_f \mathbf{Y}_f) \qquad (3.1.10)$$

$$\mathbf{Z} = \mathbf{D}^{-1} (\mathbf{p}_z - \mathbf{D}_f \mathbf{Z}_f)$$

Thus, member forces can be derived by:

$$\mathbf{s}=\mathbf{Lq} \qquad (3.1.11)$$

Given the external loads, the branch-node matrix, force densities and fixed degrees of freedom, we can determine a set of free nodal coordinates by solving the equation 3.1.11.

General workflow of FDM is shown in Figure 4. The input of the FDM functions are bar network or line mesh in 2D with their connectivity, force densities of each line/bar, nodal load at each node may it be in x, y or z direction, support points or fixed point and further constraints as mentioned in (Schek, 1974). The result of FDM will give nodal points, which are at equilibrium as per given input values. The bar nodes connected will give final structural layout in 3D. Forces in each member is calculated by product of force density with length of the member squared. Thus, form found structure need to be further analyzed for other load cases, global stability, buckling and other requirements.

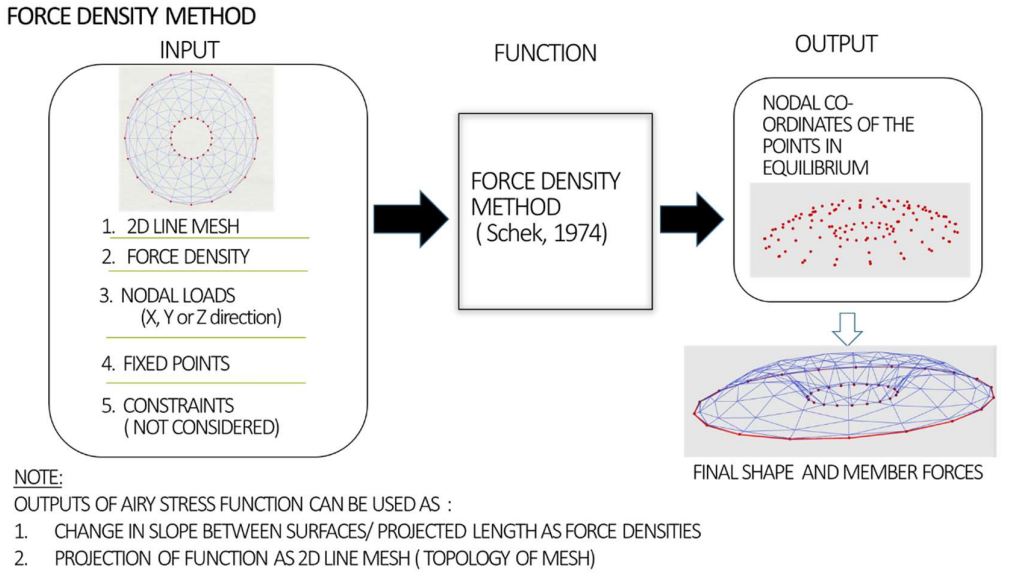

Figure 4 Force Density Method workflow

3.2 Validation of FDM formulation

Validation of FDM formulation has been done by comparing the forces in the members obtained from FDM with FEM software ETABS. First, Form finding of a pin connected line like bar network with member connectivity as in Figure 5 and force density values and nodal loads from Table 2 is done. Then, the grid shell geometry is analyzed in ETABS with same nodal loads and support conditions. Details of the modeling are present in Table 2.

Table 2 Parameters for FDM and FEM

FEM Modeling software:	ETABS 18
Bar material:	MS (Fe 250)
Bar section:	ISNB40M (all bars)
Member end connection:	Fixed
Support connection:	Pinned
Grid shell length:	8m
Grid shell breadth:	8m
Grid shell max height:	1.74m
UDL over shell surface	5 KNm^{-2}
Nodal load:	15.26 KN (gravity load)
Force Density:	20KNm^{-1} (each member)

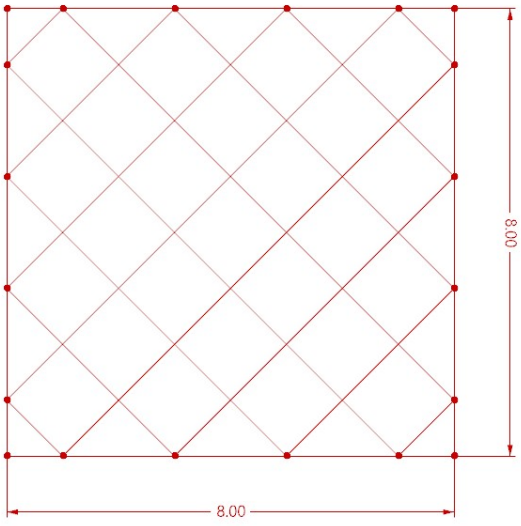

Figure 5 2D Bar network - input of FDM

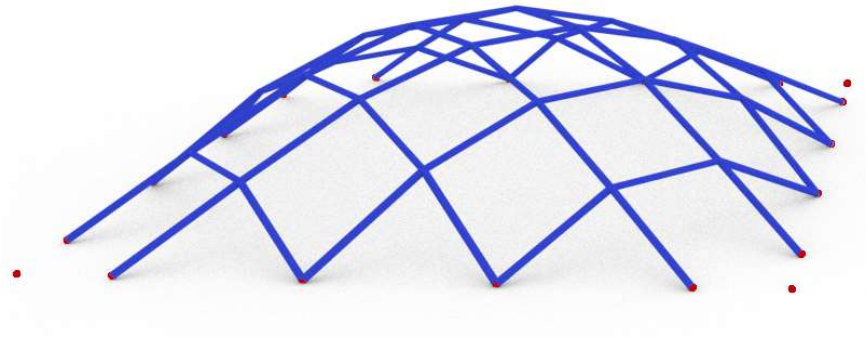

Figure 6 Form found grid shell with FDM

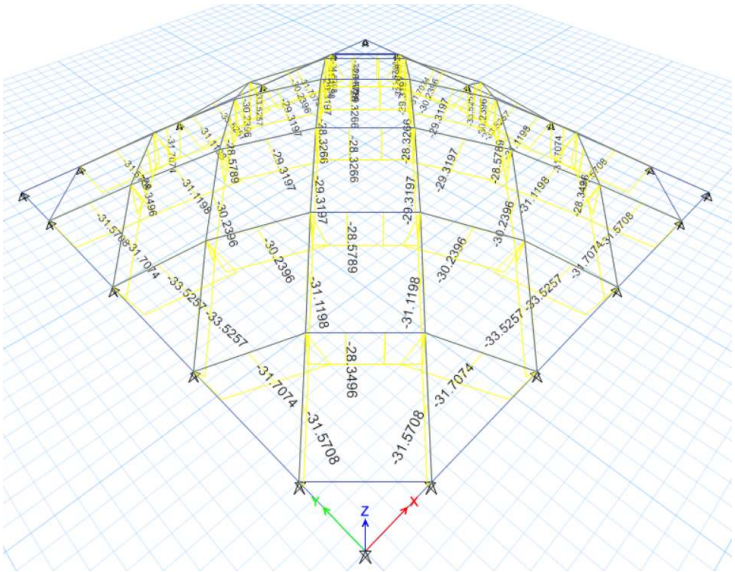

Figure 7 ETABS model of the grid shell

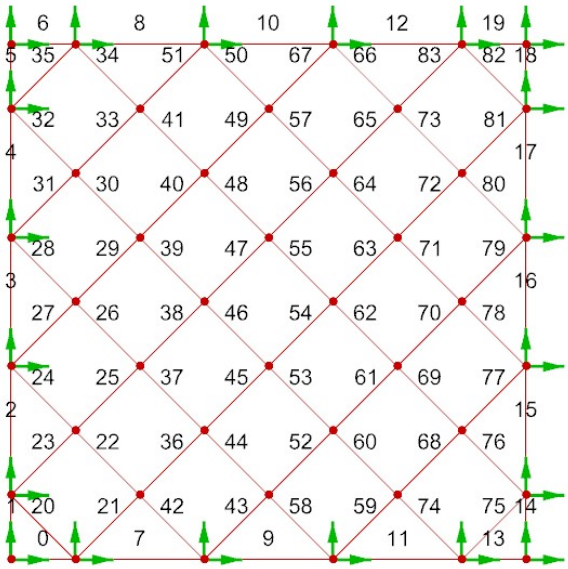

Figure 8 Plan view of grid shell with member labeling

Table 3 Variation in member forces between FDM and ETABS

Member Label	FDM Member forces	ETABS Member forces (KN)	Variation %
28	33.19	33.53	1.01
29	29.92	30.24	1.06
30	31.61	31.12	-1.57
31	31.14	31.7	1.77
32	31.61	31.57	-0.13
33	28.28	28.35	0.25
34	31.61	31.57	-0.13
35	0	0	0.00
39	29.29	29.32	0.10
40	28.28	28.58	1.05
41	31.14	31.12	-0.06
47	28.28	28.33	0.18
48	29.29	29.32	0.10
49	29.92	30.24	1.06
50	33.19	33.53	1.01
51	31.61	31.7	0.28

Table 3 consists of comparison of force values obtained from FDM and ETABS. Using double symmetry of the grid shell taken, comparison of forces in members within a quarter has been done and presented. From Table 3 it is seen that member force values obtained from FDM and ETABS are very close to each other, thus, validating the use of formulated FDM.

3.3 Structural weight and total load path

Grid shell members are considered to be fully stressed; thus, it is possible for representation of total structural weight by total load path of the structure. Load path for a member is given by its member length multiplied by force in the member.

Total weight of structure (W) = Σ_1^n A_i L_i ρ_i

where, n is the numbers of members, L is length and A, the area of each member, ρ density of the material used.

Considering each member to be fully stressed to stress capacity σ, $A_i = F_i / \sigma$,

Thus, W = Σ_1^n Fi Li, (ρ_i / σ). In the study, material grade is considered constant,

thus (ρ_i / σ) = constant.

i.e. $W \propto \Sigma_1^n F_i L_i$, i.e., total load path of the structure. Hence, in the study, structural weight is represented by total load path of the structure where cross section of the members is not defined.

3.4 Force density

Shape analysis of tensile structures is a geometrically non–linear problem, the FDM linearizes the form–fitting equations analytically by using the force density ratio for each cable element, q = F/L, where F and L are the force and length of a cable element respectively (Southern, 2011). Same principle holds for compression - tension and compression only structures like grid-shells. Force density of a member during FDM is assigned as per its axial strength.

For form finding of a grid shell, force density values input in FDM, are directly dependent on the choices of materials and section sizes available. For similar sectional sizes available, for material like wood, force density values assigned are lower, given their lower compressive strength, whereas higher values of force densities can be assigned for steel, given its higher material strength. Here, effect of variation of force density on shell weight and height is studied for force density ranging from $20KNm^{-1}$ to $60KNm^{-1}$.

3.5 Grid shell loading

Loads are applied as uniformly distributed static loads at member ends only. Uniformly distributed static load of $5KNm^{-2}$ is taken, which is applied to the nodes as per their tributary area. It is observed that for lower values of force densities in all topologies of grid shells considered, surface area of grid shell after form finding is significantly greater than that of original projected plan. Thus, multiple iterations are required in form finding to get actual loading after the shell assumes its shape.

Figure 9 shows loading error for quadrangular grid shell for various force density and 6 subdivisions. Figure 10 shows loading error vs no. of iterations for various grid shell topologies at force density $20KNm^{-1}$ and 6 subdivisions. It has been observed that for all grid topologies considered maximum of three iterations suffice to get loading values within error of 5% for force density values higher than $20\ KNm^{-1}$. Thus, three iterations of FDM are done to get the loading on nodal points.

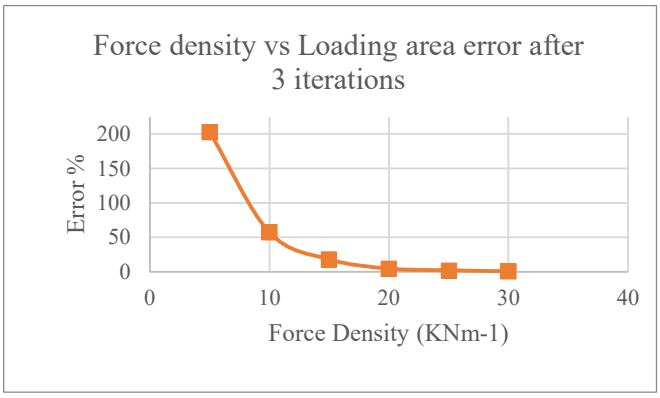

Figure 9 Loading error for quadrangular grid shell for various force density and 6 subdivisions.

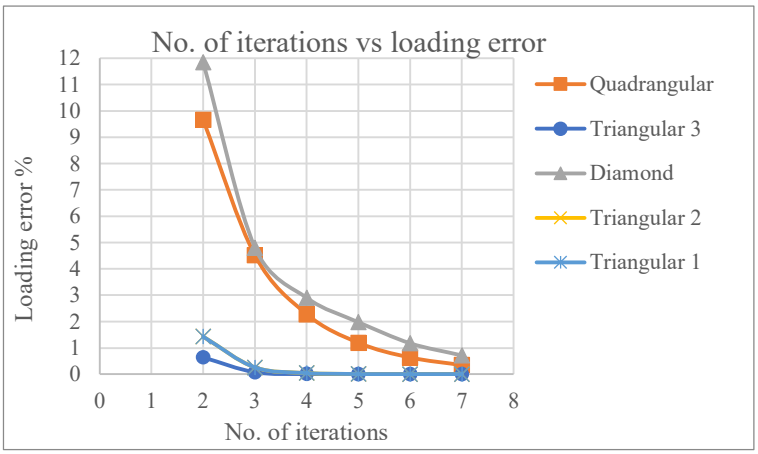

Figure 10 Loading error vs no. of iterations for various grid shell topologies at force density 20KN/m and 6 subdivisions.

Figure 11 show flowchart of methodology for grid shell form finding design and optimization using FDM. Further, Figure 12 show flowchart of methodology for grid shell design and optimization using FDM and Airy stress function. In case of methodology shown in Figure 11, first, an initial domain is constructed in 2D as per no. of subdivisions and grid topologies. FDM is used for form finding which is checked for requirements as per height limitations or max force allowed in members. In case of fulfillment of design requirements, optimization is done using genetic algorithm to get optimum grid shell as per height and weight limitations. Then, FEM is used to validate and further analyze the structure. Finally, conclusions are drawn as per results. Figure 12 shows flowchart of methodology for grid shell form finding using FDM and Airy stress function. All methodology is same as per methodology in Figure 11, but Airy stress function is used to generate force density values as input in FDM and optimization using GA is not carried out.

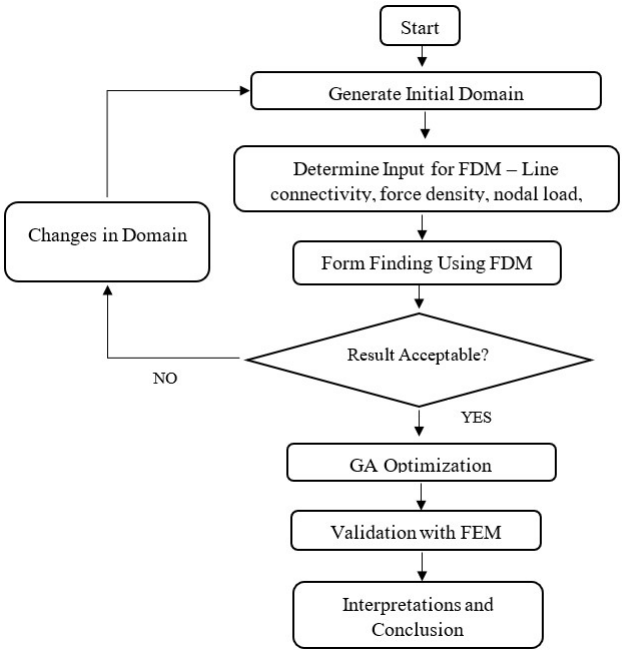

Figure 11 Flow Chart of Methodology for grid shell design and optimization using FDM.

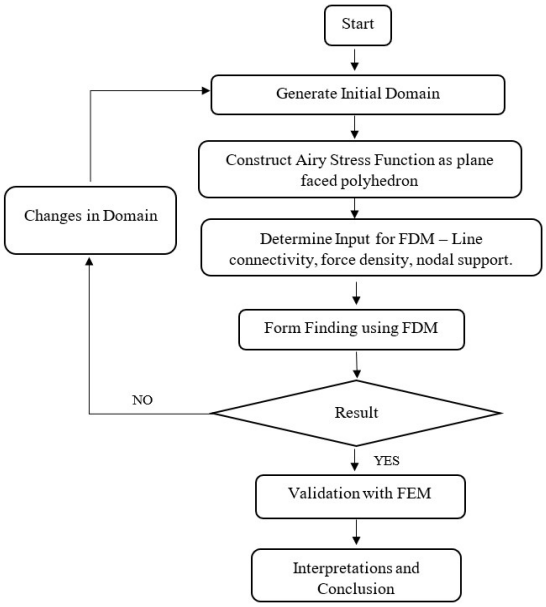

Figure 12 Flow Chart of Methodology for grid shell design and optimization using FDM and Airy Stress Function

3.6 Airy Stress Function and form polyhedron

Airy Stress Function, introduced by Airy (1862) describes the inner stresses in two-dimensional continuous structures. The stress function satisfies the governing equilibrium equations. Airy stress function can be regarded as a 3D surface $\varphi(x,\ y)$ over 2D xy-plane that contains the structure, the differentiation of which give the stresses in the plane as seen in equation 3.6.1:

$$\sigma_{xx} = \frac{\partial^2 \varphi}{\partial y^2}$$
$$\sigma_{yy} = \frac{\partial^2 \varphi}{\partial x^2} \qquad (3.6.1)$$
$$\tau_{xy} = -\frac{\partial^2 \varphi}{\partial x \partial y}$$

For polyhedral stress functions, all curvature is concentrated at the edges of the plane faces, such that the stress field is zero everywhere except along a set of discrete lines, these being the force-carrying bars of the truss (Williams & McRobie, 2016). As a result, the Airy stress function can be used for studying the static equilibrium of pin-jointed frameworks (i.e., trusses). In this case, the surface φ(x, y) is not a continuously smooth surface but a plane-faced polyhedral surface in which the curvature is zero in the planar faces that are adjacent to each polyhedral edge while the curvature change is concentrated along the edges.

In fact, 2D trusses can be seen as projections of 3D polyhedral Airy stress functions, in which the bars of the 2D structures are the projections of the polyhedral edges of the 3D stress function. The relation between Airy stress functions and equilibrium of pin-jointed frameworks was also referred by James Clerk Maxwell in his articles on graphic statics (Maxwell J. , 1870).

The angle between two adjacent faces in the 3D polyhedral Airy stress function gives the internal axial force of the corresponding bar in the 2D structure. Additionally, the local convexity of the function, which determines whether the edge of the polyhedron is convex or concave, defines if the corresponding bar in the structure is in compression or in tension respectively.

In Figure 13, φ represents the continuous airy stress function φ(x,y) in xy plane for body with force P acting along x direction over length 2B. The normal stress along x-

direction is given by partial double differentiation of stress function along y which is equal to P/b. Assumed continuous airy stress function satisfies and represents the stress condition of taken case.

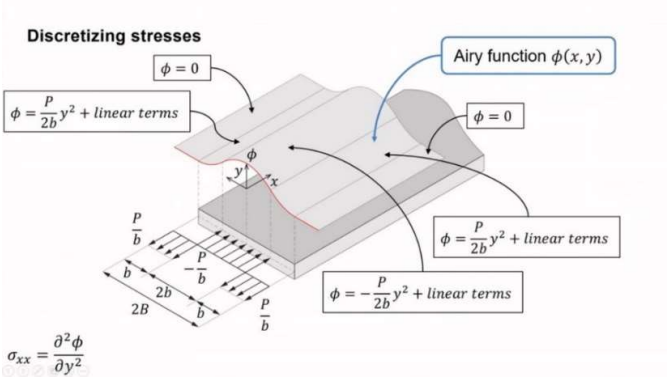

Figure 13 Continuous Airy Stress Function over continuous surface (Baker, 2021)

In Figure 14, φ represents the discretized form of airy stress function φ(x,y) . The faces of the stress function are plane, and curvature is changed only at the kinks where the total stresses are concentrated, alike to bar trusses. Assumed discrete airy stress function satisfies and represents the stress condition of taken case.

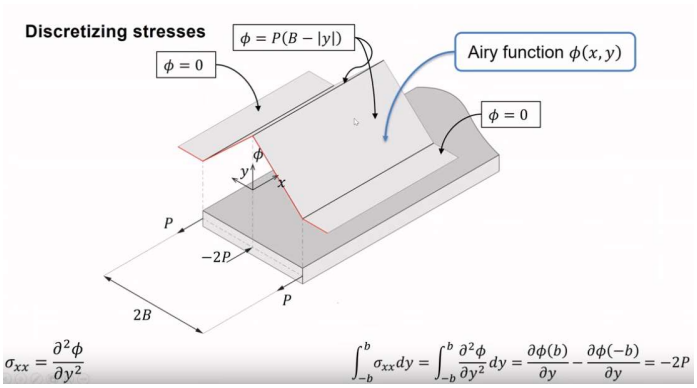

Figure 14 Discrete Airy Stress Function at intersection of two planes (Baker, 2021)

3.7 Airy Stress formulation for grid shells

Any plane faced polyhedron represents an airy stress function of a potential self-stressed pin jointed member network may it be trusses, grid shells, tensegrity structures (Mitchell, Baker, McRobie, & Mazurek, 2016). The projected network in 2d from a 3d plane faced polyhedron representing airy stress function is self-stressed i.e., that the forces in the network are in equilibrium in both plane directions (say x and y axis).

Taking the case of grid shell, a plane faced polyhedron as shown in first row Table *4*, represents an airy stress function. The 2D projection of stress polyhedron is a pin jointed bar network in 2D with same topology as of the stress polyhedron, shown in second row in Table 4. Member forces in the projected bar network can be calculated, in stress polyhedron, from the slope difference between adjacent faces of the edge, which projected is the bar network in 2D. Now, with member force and member length in 2D, one can determine the force density. FDM can be applied to the 2D network to generate grid shell with force density values obtained and chosen support and nodal loading condition. Thus, Airy stress functions can be used as topology and force density input of FDM producing a grid shell that is self-supporting in xy plane, shown in third row in Table 4. Form found shells in this way need to be checked further for global stability, performance in lateral loads and other parameters which is not in the scope of the study.

Table 4 Reciprocity of Airy Stress Function and Grid shell geometry.

Figures	Description
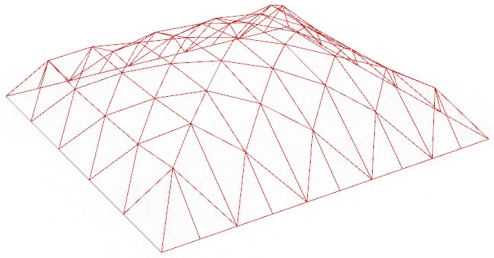	Discretized airy stress function in form of closed plane faced polyhedron. Note that the stress polyhedron is closed, hence boundary conditions satisfied and within the structure itself.
Projection	
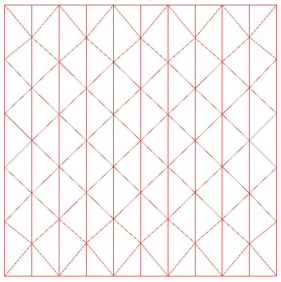	Projected plan view of stress polyhedron. Force in a projected member of an edge in stress polyhedron is given by slope difference between adjacent faces. Force density = Member Force/ Member length.
FDM	
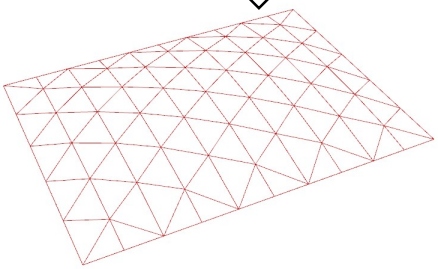	Resulting grid shell geometry with support conditions at edges obtained with FDM for force density values obtained from stress polyhedron. The structure is in equilibrium and requires no horizontal support (self - supporting)

Self-stressed structures are highly valuable in cases where constructions are required to be done for historic or masonry structures which are strong in vertical direction but have little lateral load carrying capacity.

Airy stress function in form of plane faced polyhedron and the resulting grid shell are reciprocal in nature i.e., the resulting grid shell can be used as an airy stress function to generate grid shell with form like initially taken plane faced polyhedron representing airy stress i.e., the process followed in Table 4 can be reversed taking stress polyhedron as shown in third row in Table 4 to generate grid shell geometry resembling to first row in Table 4. Thus, representing reciprocal nature as mentioned by Maxwell (1870).

3.8 Genetic Algorithm

Genetic Algorithms (GAs), based on the principle of evolution is a stochastic method. In this method, best individuals, as per their fitness (here minimum structural weight) are chosen from a random population of individuals (here grid shells) with various gene sets (here topology, force density and subdivisions) are chosen for reproduction and with specific crossing techniques, solutions are combined to bring new offspring and in that way for a new generation (Dimcic & Knippers, 2011). Crossing methods are programmed to ensure conservation of good genes and addition of mutation algorithms enable random alteration of genes thus enabling convergence towards best fit solution. New generations are produced until a satisfactory result is found. In our case, the satisfactory result is statically stable grid-shells with minimum weight for various height configurations. More on application of GAs can be found in (Goldberg & Holland, 1988).

This process is very similar to natural selection in the real world since Galapagos iterates, or breeds, multiple generations of solutions until it finds what it believes to be the fittest solution. Figure 15 shows the basic genetic algorithm process.

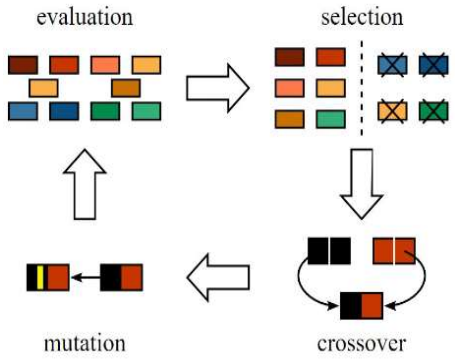

Figure 15 General overview of Evolutionary solver mechanism (Cheng, 2018)

Two cases are examined for optimization, one being minimum grid shell weight without any regards for height and second minimum grid shell weight for height equal to 1.5m. For weight minimization with limit on height of 1.5m, the objective function for minimization is set as:

Minimize, W = Σ_1^n FiLi∗(h-1.5)^2,

where, F_i = force in individual member

L_i = member length

h= grid-shell height obtained

n = no. of members.

In this thesis, we will be using Galapagos Solver, in-built plugin in Rhino-Grasshopper.

Figure 16 presents basic workflow for grid shell design using FDM only and FDM with Airy Stress Function.

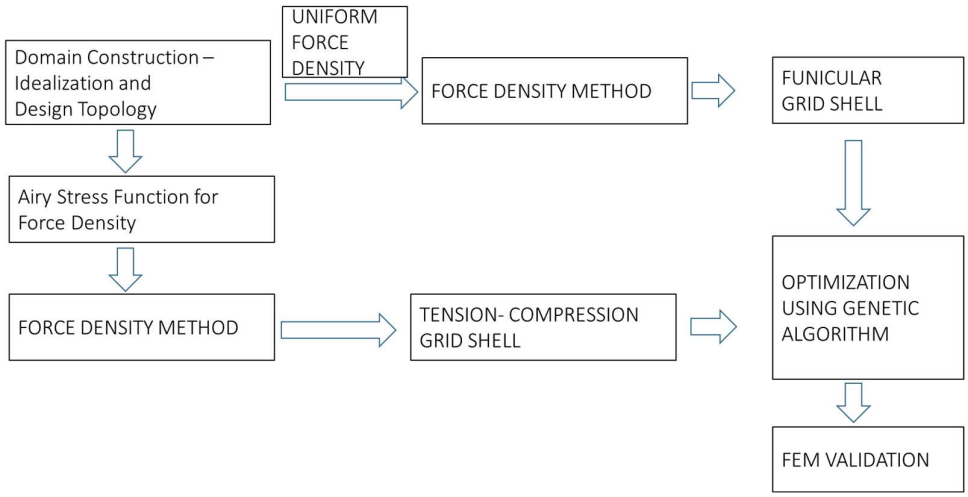

Figure 16 Basic Workflow for grid shell design using FDM only and FDM with Airy Stress Function.

CHAPTER 4: RESULTS AND DISCUSSIONS

Results and discussions are divided into three parts.

1. Form finding of arbitrary shell boundary shapes - the general ability of design tool formulated is shown.
2. Study of variation of weight, height, and deflection of a 12m * 12m grid shell – Parametric variation of shell height, weight and deflections are studied for mentioned grid shell with variations in topology, grid density and force density.
3. Design of self-supporting grid shell using Airy stress function – Airy stress function is used in conjunction with force density method to generate self-supporting (laterally) grid-shell forms. The resulting shapes are compared to the grid-shells, form found using FDM method only.

4.1 Form finding shells with irregular boundary shapes

Grid shells allows for compatibility and efficiency of load transfer even in areas with highly irregular geometrical plans. This ability to span over areas with irregular boundaries and support conditions is an advantage not provided by other spanning or roofing structures. At early phases of design, determination of grid shell geometry is crucial as it dictates the rest of the design. A design tool has been formulated that determines shell geometry in static equilibrium as per the conditions of grid densities, topologies preferred and construction material (represented by force density). Following are some shell geometries for irregular plan and support configurations obtained using FDM formulation in Rhino-Grasshopper.

Table *5* shows various grid shell geometries obtained varying the parameters in FDM for two types of arbitrarily chosen grid-shell plan geometries. Boundaries are represented by red lines and supports as red dots and resulting grid shell by blue lines.

Table 5 Variations of grid shell geometries obtained for boundary (red line) and support (red dot) for various grid densities, force densities and topologies.

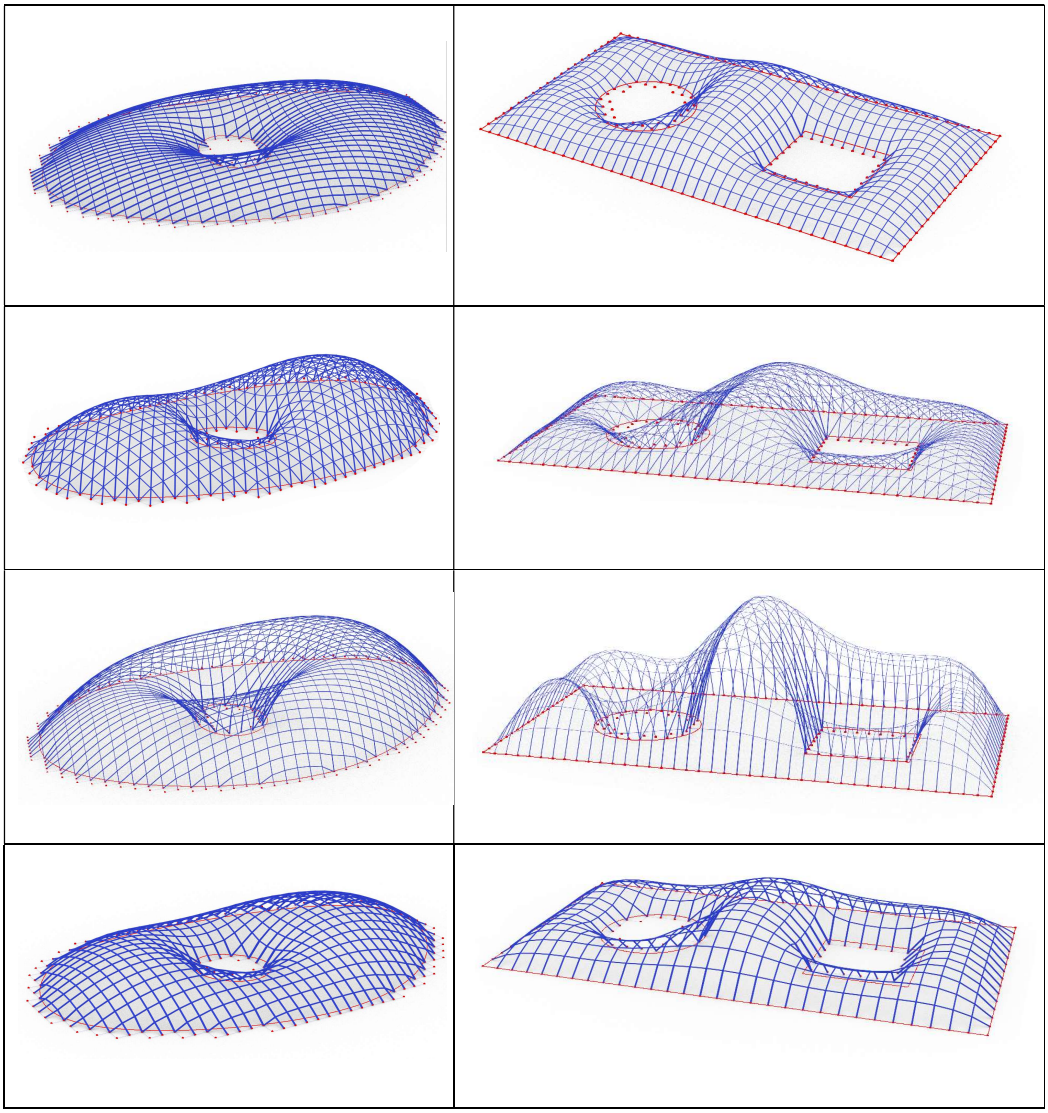

First row in Table 5 shows a grid shell obtained with arbitrary shape, force density values and grid densities. In second row, the grid mesh is triangulated. In third row, force density values are reduced by half. In third row grid density is decreased from the first by seventy five percent. The resulting grid shells are in static equilibrium and further analysis for global stability, other load cases need to be performed for finalization of design. However, starting from form found geometry as above in comparison to arbitrary shapes take, would certainly be beneficial to obtain economic and structurally sound design.

4.2 Parametric variation in weight, height and deflection using FDM

Case study of a 12m x 12m span covering grid shell with pin support on all the edges is done. Variation of structural weight, represented by total load path, corresponding height, and maximum deflection of grid shell as per variation in parameters listed below are studied:

- Topology – quadrilateral grids (quadrangular and diamond shaped) and triangular grid of 3 types as shown in Figure 17.
- Grid density or number of subdivisions of span ranging from (6 to 24)
- Force density ranging from (20 KNm^{-1} to 60 KNm^{-1})

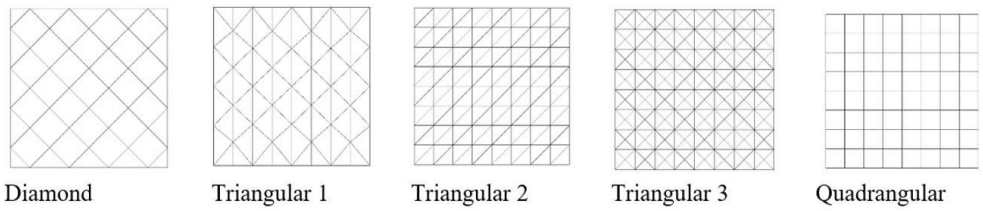

Figure 17 Grid shell typologies considered in study.

Table 6 shows variation of total structural weight, grid shell height and maximum deflection for five different grid topology types, keeping no. of subdivisions equal to 8 and constant force density of 25KNm^{-1}. From the table among considered grid types, quadrangular has lowest structural weight (57%) of highest which is triangular type 1 and 3. At the same time, triangular type 3 has the lowest grid shell height (37%) of the diamond type. From Table 6, among other grid types, quadrangular and diamond types have lower structural weight, because of lower value of load path, as fewer members transfer the forces to the support.

Table 6 Grid shell height, weight and deflection variation for variation in topology for 8 no. of divisions and force density 25KN/m.

Grid Type	Load path (KNm)	Normalized load path	Shell height (m)	Normalized shell height	Shell deflection (mm)	Normalized shell deflection
Diamond	8617.82	0.61	3.31	1.00	2.68	0.63
Triangular 1	13962.97	1.00	1.54	0.46	2.81	0.66
Triangular 2	13706.90	0.98	1.53	0.46	4.28	1.00
Triangular 3	14017.73	1.00	1.24	0.37	2.49	0.58
Quadrangular	7984.91	0.57	3.26	0.98	1.14	0.27

Further, it has been seen that Triangular 2 type topology grid shell attains the maximum deflection and Quadrangular type having the minimum i.e., 27% of the maximum value for taken conditions of 8 numbers of subdivisions and 25KNm^{-1} uniform force density. Besides the maximum and minimum deflection values rest have similar magnitude. The co-relation of deflection with topology is not found to be direct and further study is required.

From Figure 18 it is observed that keeping force densities constant for grid shell topologies, increase in grid density i.e., no. of subdivisions reduces the shell height considerably at lower values of subdivisions whereas, the changes are less pronounced at higher values. From Figure 18 it is seen that, quadrilateral type grid topologies i.e., quadrangular and diamond types exhibit similar variation, and all the triangular topologies have alike variation in height for variations in grid density with constant force density.

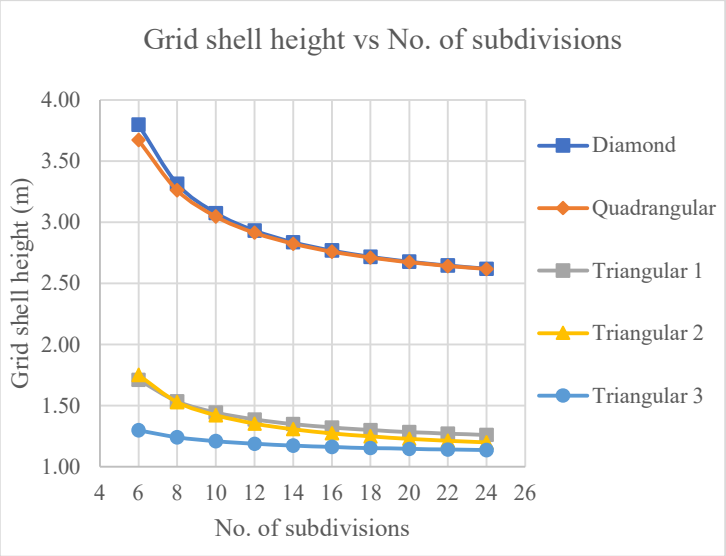

Figure 18 Variation of grid shell height as per grid density for force density of 25KN/m.

Figure 19 shows that increasing sub-divisions increase grid shell structural weight for triangular type grid shells. In quadrangular type, grid shell weight decreases at lower values with rise in subdivisions assume almost constant value. In diamond type grid shell, it is seen that increasing subdivision decreases shell weight considerably at lower values and assumes almost constant value at higher subdivisions alike quadrangular type.

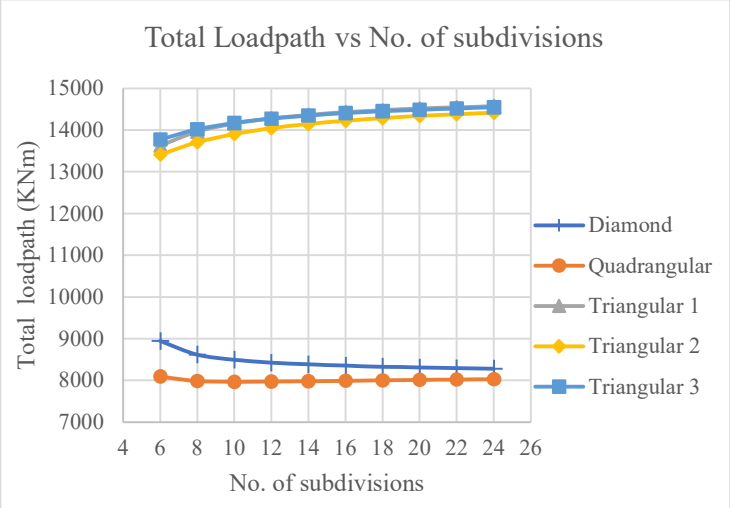

Figure 19 Variation of grid shell structural weight as per grid density for force density of 25KN/m.

Figure 20 shows variation of grid shell deflection for various shell subdivisions at constant for density value of 25KNm^{-1}. It is observed that triangular 2 type grid shells have highest deflection while quadrangular type has the lowest. For rest of topologies the deflections variation with subdivisions are alike.

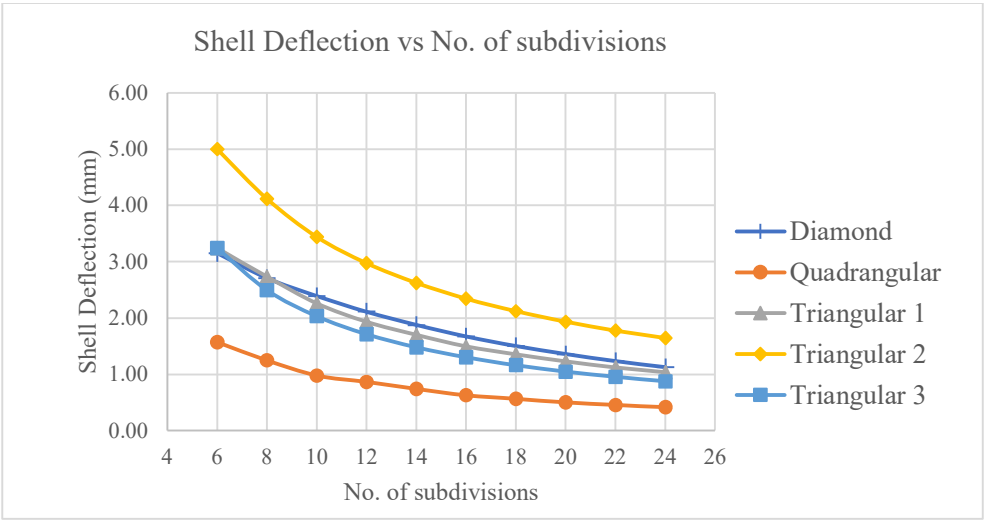

Figure 20 Variation of grid shell deflection with numbers of subdivision for force density of 25 KN/m.

For all grid shells, variations of height, weight and deflections with subdivisions are more pronounced at lower values of subdivisions but at higher values the grid shell weight variation with subdivisions is subdued. This decreased variation in height,

weight, and deflection of grid shell as grid density is increased can be explained by the fact that as we approach higher no. of subdivisions the grid shell assumes almost continuous surface with regular curvature. In lower subdivisions adjacent panels are highly irregular and even the small increment in subdivision makes more impact in making shell more regular. However, at higher subdivisions grid shell is almost regular and changes in subdivision have little or no impact in overall structural characteristic.

In next case, for a 12m x 12m grid shell with 12 numbers of subdivisions at support and various topologies, variation of grid shell height and structural weight is determined with respect to force density. Figure 21 shows that at lower values of force densities structural height reduce highly with increase in force density whereas for higher values of force densities, the rate of change of structural height is decreased highly assuming almost linear variation. Further, Figure 22 shows linear variation of grid shell structural weight with force density for triangular type grid shells. This linearity in quadrilateral type topologies is observed at higher values of force density with slight kink at the lower value.

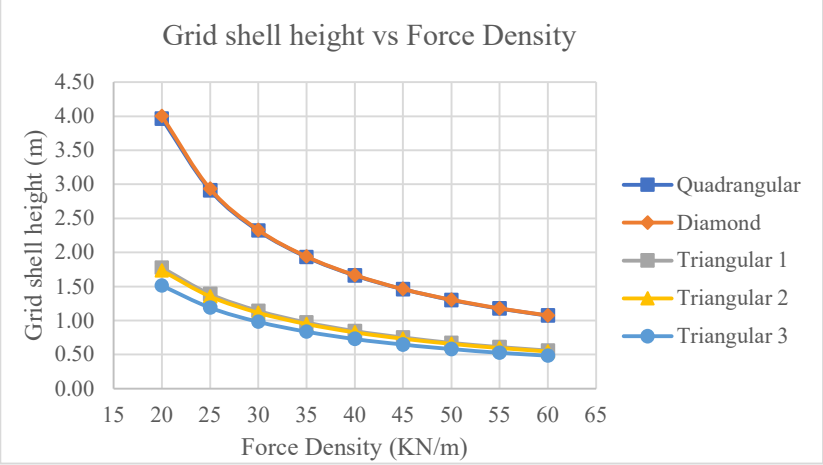

Figure 21 Variation of grid shell height as per force density for 12 subdivisions.

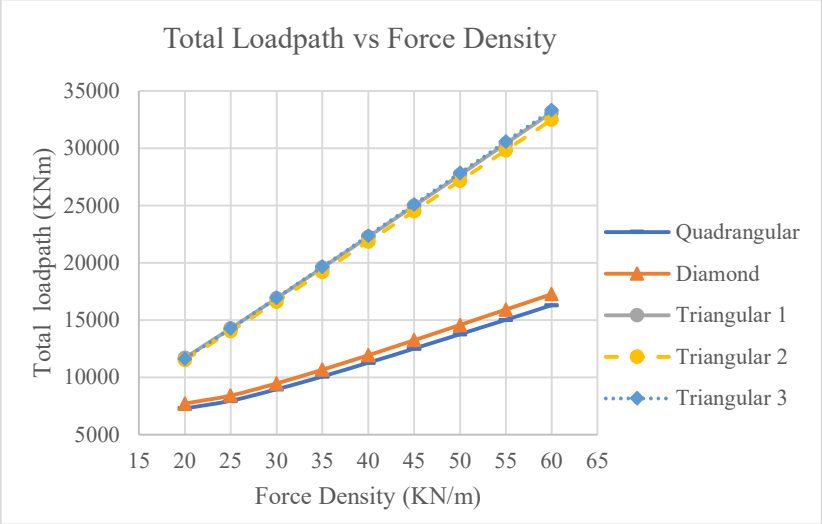

Figure 22 Variation of grid shell structural weight as per force density for 12 subdivisions.

The relation of force density and maximum deflection for 12 subdivisions and various topologies is shown in Figure 23. It has been observed that, increasing the force density increases the shell deflection. This is more pronounced for Triangular 2 type grid shell and less for triangular 3 type topology, while rest showing similar variation. The increasing amount of deflection at higher force density can be attributed to the observation that as force density values are increased there is subsequent decrease in shell height. As shell height decrease, for the same loading, axial thrust in members increase, increasing strains and thus deflection in vertical direction as well.

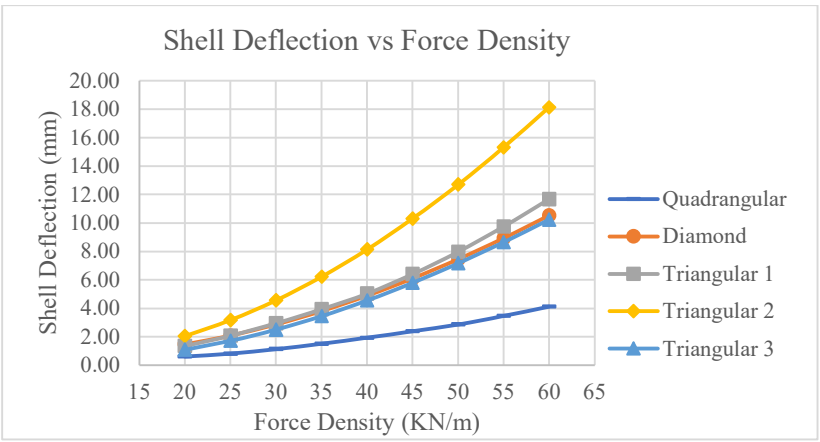

Figure 23 Variation of grid shell structural weight as per force density for 12 subdivisions.

4.2 Optimization for weight and height

The results of the case study show opposite variation of structural weight and height, for each of the parametric variation. Thus, optimization seems logical for the determination of case that satisfy both parameters. Results from genetic algorithm shows the value of optimum value of grid shell height and structural weight for given parameters as seen in Table 7.

Table 7 GA Optimization result for structural weight and height

S.no.	Cases	Grid type	No. of subdivisions	Total load path (KNm)	Structural height (m)	Force density (KN/m)
1	Minimize Structural weight	Quadrangular	24	7136.3	3.51	20
2	Height =1.5m	Triangular 3	14	11700.76	1.49	20

From optimization of the grid shell for minimum values of structural weight and height it is observed that quadrangular type grid shell has lowest structural weight when no height limitation is imposed. The grid shell structure obtained from the optimization are presented in the Figure 24. Furthermore, grid type topology of triangular 3 has lowest structural weight with total load path of 11700.76 KNm when height limitation of 1.5m is imposed. The grid shell obtained is presented in Figure 25.

It has been observed that quadrilateral type grid shells, in comparison to triangular type grid shell topologies, have lower structural weight when no height limitations are imposed. However, given the non-planarity of panels, the fabrication costs are higher. Thus, further studies can be done, to obtain planar faced grid shells and then compare the results with triangular grid types in which planarity is inherent.

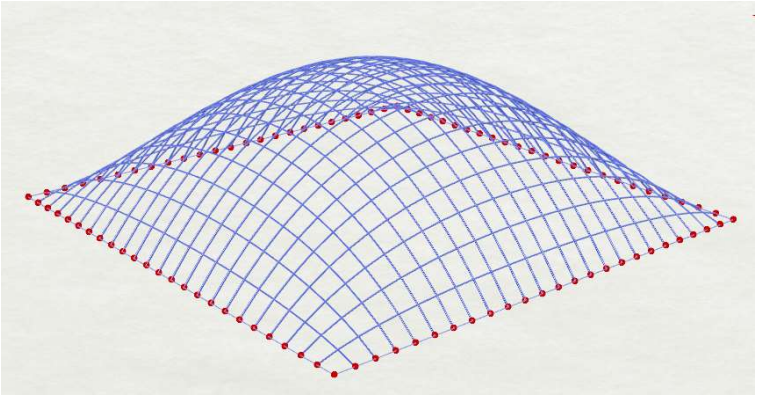

Figure 24 Grid shell form obtained for minimum structural weight as per case 1.

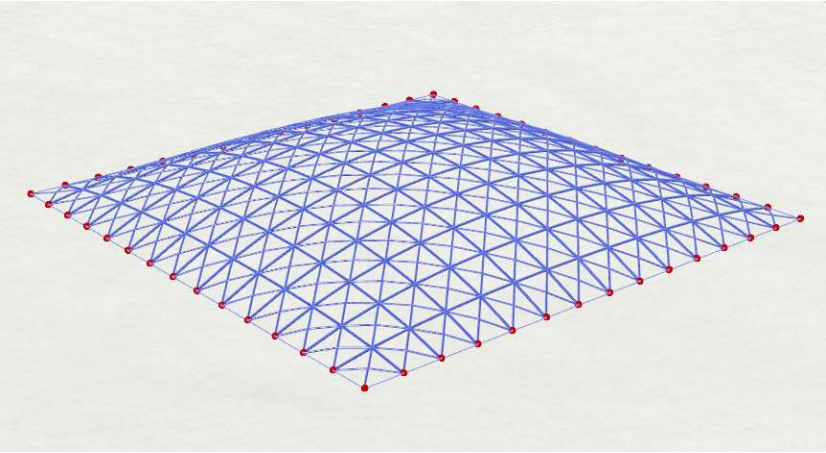

Figure 25 Grid shell form obtained for grid shell height of 1.5m as per case 2.

4.3 Discrete Airy stress function and FDM

Two self-stressed grid-shells whose forms are determined using airy stress function and FDM are studied and presented below with comparison of grid shells with similar nature form found using uniform force density for all members. The results and steps followed are presented below.

4.3.1 Rectangular plan grid shell

Steps followed for comparison between grid shell geometries obtained from FDM alone and FDM in conjunction with stress polyhedron are given below:

1. Construct Airy Stress Function (Plane faced polyhedron)
   1.1 Take grid shell plan with appropriate meshing.
   1.2 Determine the grid shell form using FDM with support along the boundary, resulting grid shell is taken as stress polyhedron.

2. Determine Force Density values of each member from plane faced polyhedron.
3. Take projection of Plane faced polyhedron to get bar network (input for FDM) and determine slope difference between two plane faces (values representing force densities).
4. Determine grid shell form with supports as required using bar network, support condition and force density values. In this case support are taken to be at corners only.

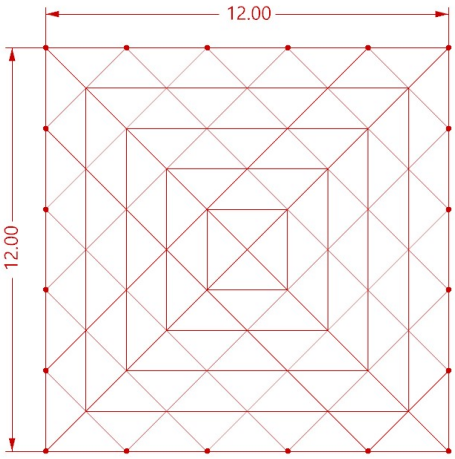

Figure 26 Grid shell plan with supports and member connectivity

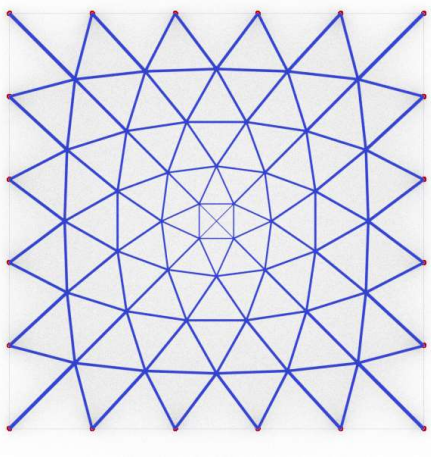

Figure 27 Plan view of Grid shell after form-finding with FDM (FD = 15 KN/m)

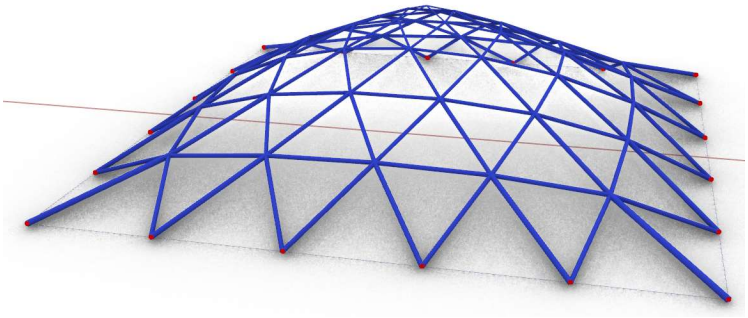

Figure 28 Perspective view of Grid shell after form-finding with FDM (FD = 15 KN/m)

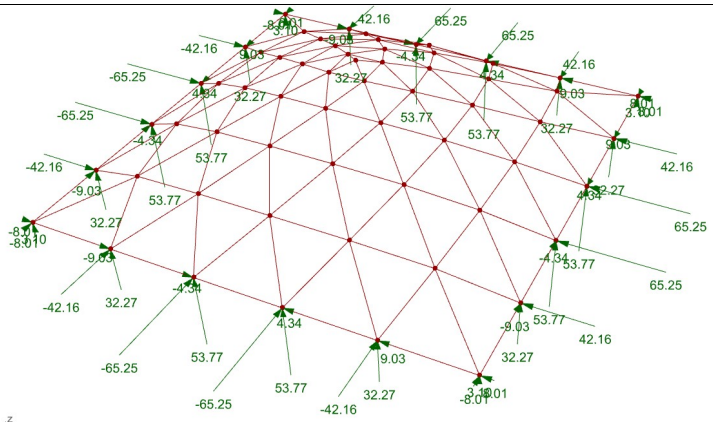

Figure 29 Perspective view of Grid shell support reaction (Reaction units in KN)

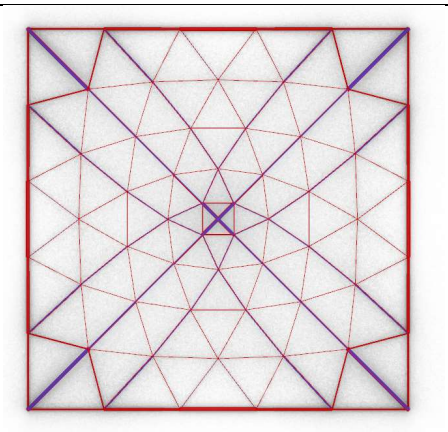

Figure 30 Plan view of Grid shell after form-finding with force density values input from Airy Stress Function taken to be grid shell form at Figure 28

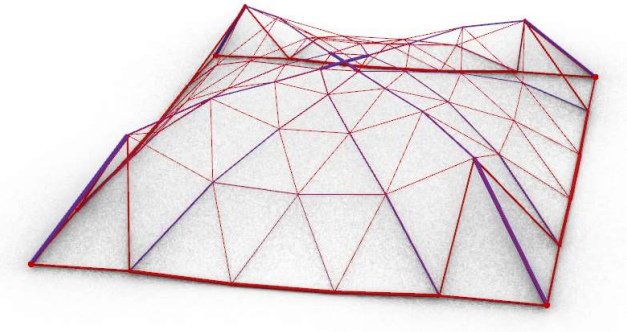

Figure 31 Perspective view Grid shell after form-finding with force density values input from Airy Stress Function taken to be grid shell form at Figure 28

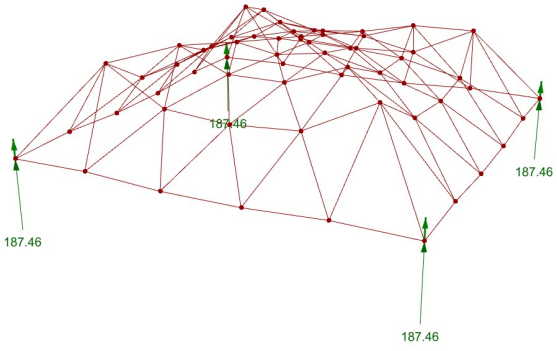

Figure 32 Perspective view Grid shell and support reactions after form-finding with force density values input from Airy Stress Function taken to be grid shell form at Figure 28

Table 8 presents comparison between basic parameters of grid shell geometries obtained using FDM alone and FDM in conjunction with Airy Stress function. Comparison between grid shells with same height is taken.

Note that there are not any horizontal reactions for vertical loading in the supports in case II. Thus, roof isolation could be achieved with limited load transferred to the substructure. Further study needs to be done for lateral load cases of wind and earthquake to finalize the design.

Table 8 Comparison of basic parameters using FDM and FDM along with stress polyhedron for rectangular plan grid shell.

Parameter		**Case I - FDM**	**Case II - FDM + AIRY**
Structural weight	Kg	1149.25	1852.6
Shell height	M	2.89	2.85
Vertical deflection	mm	5	98
Fundamental time-period	S	0.042	0.27
Force Type		Compression only	Both Compression and Tension
Minimum force in member	KN	9.86	-9.83 (Compression)
Maximum force in member	KN	44.1	-261.53 (Compression)
Members used		ISNB40M, ISNB50M	ISNB40M, ISNB50M, ISNB80M, ISNB110M
Reaction Type		Reaction along all three axes at each support.	Reaction only along z axis at all support.
Grid shell Geometry		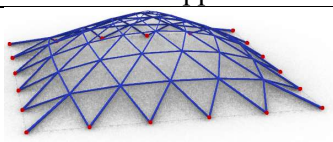	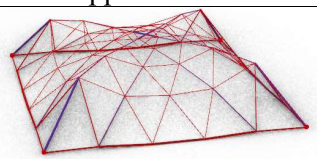

4.3.2 Circular plan grid shell

Steps followed for comparison between grid shell geometries obtained from FDM alone and FDM in conjunction with stress polyhedron for a circular plan grid shell with opening in middle are given below:

1. Construct Airy Stress Function (Plane faced polyhedron). In this case done revolving a circular arc about z axis as shown in Figure 33 to Figure 35 .

2. Determine Force Density values of each member from plane faced polyhedron.
3. Take projection of Plane faced polyhedron to get bar network (input for FDM) and determine slope difference between two plane faces (values representing force densities).
4. Determine grid shell form with supports as required using bar network, support condition and force density values. In this case support are taken to be at nodes at inner and outer boundaries of the area considered.

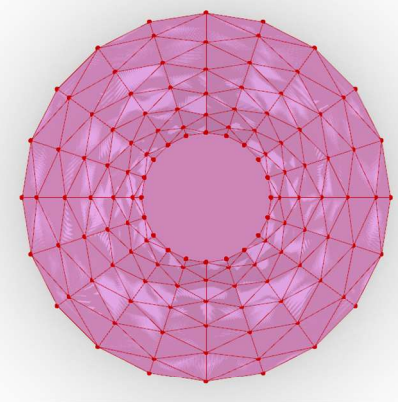

Figure 33 Plan view of stress polyhedron for circular type grid shell

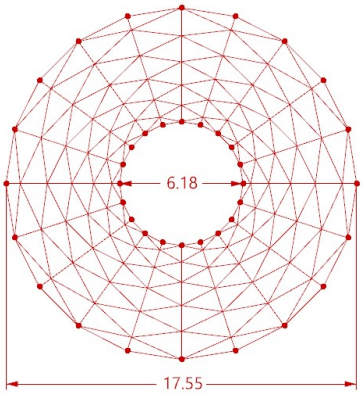

Figure 34 Projection of stress polyhedron of circular type grid shell representing base geometry for FDM

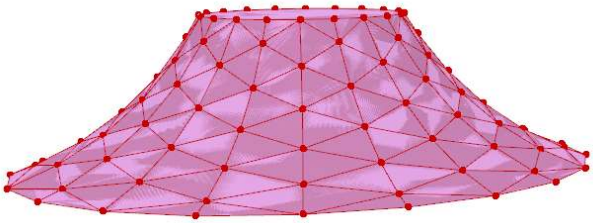

Figure 35 3D view of stress polyhedron for circular type grid shell

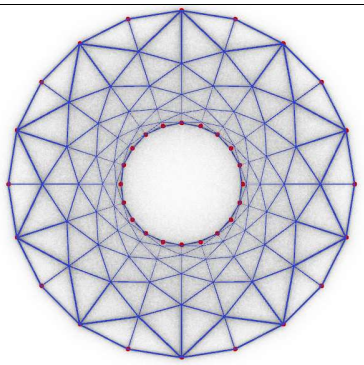

Figure 36 Plan view of grid shell geometry obtained from FDM using uniform force density.

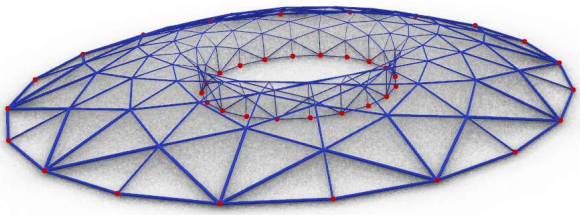

Figure 37 3D view of grid shell geometry obtained from FDM using uniform force density.

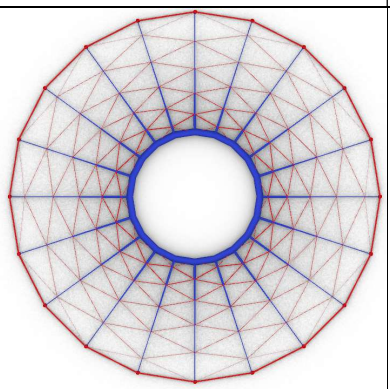

Figure 38 Plan view of grid shell geometry obtained from FDM using force density values from stress polyhedron.

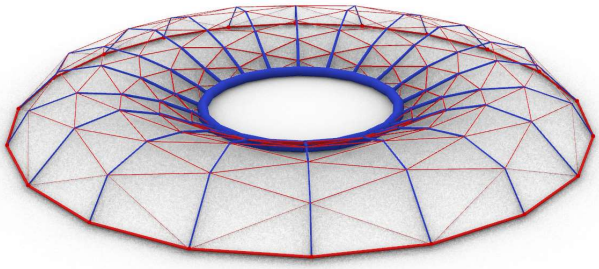

Figure 39 3D view of grid shell geometry obtained from FDM using force density values from stress polyhedron.

Table 9 compares two grid-shell parameters of similar height and base dimensions. The resulting structural weight is found to be similar. The deflection for grid shell form found using stress polyhedron and FDM is found to be higher, although within allowable limit. Grid shell form obtained using stress polyhedron and FDM is self-supporting in lateral direction, thus, limiting the forces in supports. However, to achieve this, the grid-shell undergoes in tension-compression in contrast to only compressive force in grid-shell obtained using uniform force density alone.

Table 9 Comparison of basic parameters using FDM and FDM along with stress polyhedron for circular plan grid shell

Parameter		**CASE I (FDM)**	**CASE II (FDM + AIRY)**
Structural weight	Kg	2102	2120
Shell height	M	1.39	1.37
Vertical deflection	mm	16	38
Fundamental time period	S	0.053	0.047
Force Type		Compression only	Both Compression and Tension
Maximum Compressive force in member	KN	46.7	168.69
Maximum Tensile force in member	KN	-	38.12
Members used		ISNB40M, ISNB50M	ISNB40M, ISNB65M
Reaction Type		Reaction along all three axes at each support.	Reaction only along z axis at all support.

In case of circular grid-shell with oculus in middle, the basic parameters of two grid-shells for static gravity loads are similar, however, self-supporting behavior is the major advantage of grid-shell in case II because it would reduce strength required at supports thus making overall design more economic.

4.3.3 Structures obtained by variation of support condition

Generation of several structures in equilibrium, as shown in Table 10, is possible by varying support condition in the same airy stress polyhedron as shown in Figure 28. The support conditions are varied in each row and force density values scaled by same value. Note that the structure is in static equilibrium with vertical members shown blue in compression and edge (peripheral) members at top in red in tension. It presents abundant design freedom, with possibility of numerous explorations of structures at early design phase, at the same time satisfying basic structural constraints, enabling more economic and optimized structures.

Table 10 Various shapes generated from Airy Stress Function

Member network in 2D as projection of plane faced polyhedron. Support is shown as dot.	Compression -Tension Pin joined structure obtained with given airy stress function and support condition.
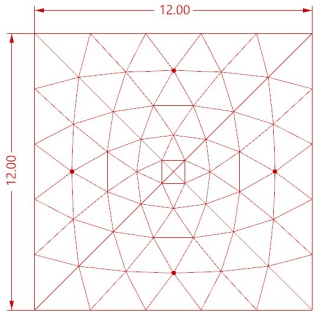	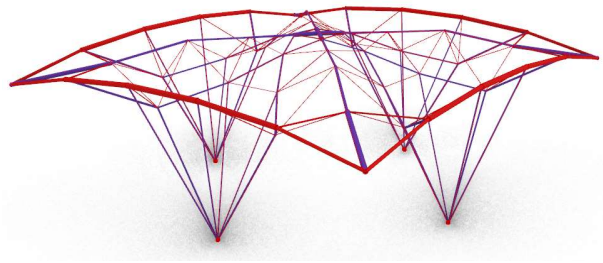
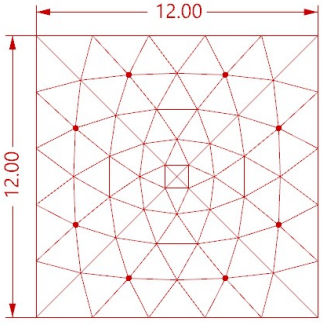	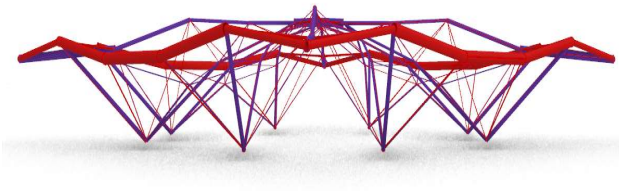
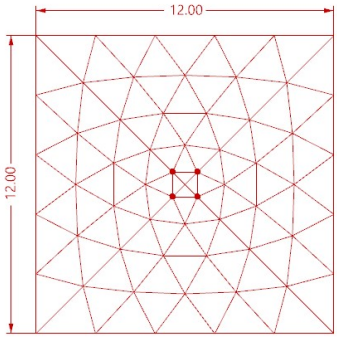	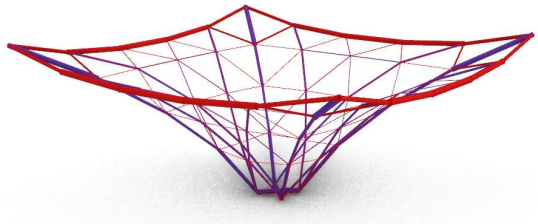
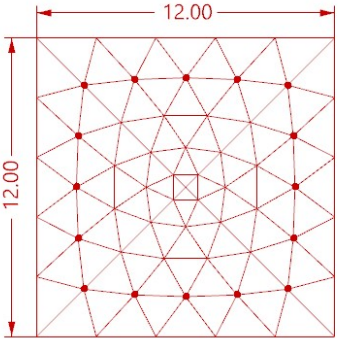	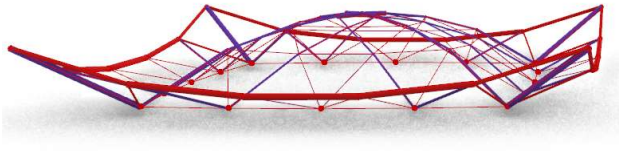

CHAPTER 5: CONCLUSION

5.1 Conclusions

In this study, FDM along with discrete form of airy stress function has been utilized for design and optimization of grid-shells. A design tool for form finding and optimization at early design stage is created and, using the same, case study of a 12m x 12m rectangular plan grid shell has been done for various topologies, grid densities and force density values.

The FDM formulation has been validated against FEM model with errors within acceptable limits. Furthermore, GA has been employed to determine the optimum structural weight and height within the given limits. It has been observed, that for cases with no height limitation of grid shells, quadrangular followed by diamond shape grid type among other grid types have lowest structural weight whereas, triangular grid shapes generally have lowest height, although having higher structural weight. Optimization is generally case specific and required for each individual case. However, the study provides general outline to achieve economy in design.

Discrete Airy Stress Functions in form of plane faced polyhedrons have been used to generate grid shell structures self-supported in lateral directions for various support conditions. It has been found that, use of airy stress function can be done to generate self-supporting grid shell structures with structural performances similar to funicular structures. Even though, such structures have generally higher material requirements, they can be used in cases where roofing substructures are unable to sustain lateral loads such masonry structures.

5.2 Further recommendations

1. It is recommended to consider lateral loads and other load cases for optimization.
2. During form finding, in case of quadrilateral shell topologies, use of constraints in FDM can be done to generate constant lengths or plane panels, conditions, which are more suitable for fabrication.
3. Discrete airy stress functions taken for comparison in this study are of single type for both rectangular and circular case. Parametric variations can be done to generate various stress polyhedron, which can be analyzed to get optimum grid shells.

REFERENCES

Adriaenssens, S., Block, P., Veenendaal, D., & Williams, C. (2014). *Shell structures for architecture: form finding and optimization.*

Airy, G. (1862). On the Strains in the Interior of Beams. *Philosophical Transactions of the Royal Society of Lodon*, 153:49–79.

Baker, W. F. (2021, August). *SpatialStructures2021*. Retrieved from youtube.com: https://www.youtube.com/watch?v=x5XcUG99eIA&t=1210s

Beghini, L., Carrion, J., Beghini, A., Mazurek, A., B. W., & and Carrion, J. (2014). Structural optimization using graphic statics. *Springer, 49*(3), 351-366.

Block, P., & Ochsendorf, J. (2007). Thrust network analysis: a new methodology for three-dimensional equilibrium. *Journal of the International Association for Shell and Spatial Structures*, 167-173(7).

Block, P., DeJong, M., & Ochsendorf, J. (2006). As Hangs the Flexible Line: Equilibrium of Masonry Arches. *Nexus Network Journal 2006 8:2, 8*(2), 13-24.

Cercadillo-García, C., & Fernández-Cabo, J. (2016, 4). Analytical and Numerical funicular analysis by means of the Parametric Force Density Method. *Journal of Applied Research and Technology, 14*(2), 108-124.

Cheng, J. (2018). *strong.io*. Retrieved from https://www.strong.io/blog/evolutionary-optimization

Coelho, R., Tysmans, T., & Verwimp, E. (2014). Form finding & structural optimization: A project-based course for graduate students in civil and architectural engineering. *Structural and Multidisciplinary Optimization, 49*(6), 1037-1046.

Dimcic, M., & Knippers, J. (2011). Free-form Grid Shell Design Based on Genetic Algorithms. (pp. 272-277). Association for Computer Aided Design in Architecture.

Fraternali, F. (2010). A thrust network approach to the equilibrium problem of unreinforced masonry vaults via polyhedral stress functions. *Mechanics Research Communications, 37*(2), 198-204.

Glass roof Dutch Maritime Museum at Amsterdam, Netherlands. (2017). Retrieved from https://ney.partners/project/glass-roof-dutch-maritime-museum/

Goldberg, D., & Holland, J. (1988). Genetic algorithms and machine learning. *Kluwer Academic Publishers*.

Grande, E., Imbimbo, M., & Tomei, V. (2018). Structural Optimization of Grid Shells: Design Parameters and Combined Strategies. *Journal of Architectural Engineering, 24*(1).

Green, H., & Lauri, D. (2017). *Form Finding of Grid Shells - a Parametric Approach using Dynamic Relaxation.* Thesis, Royal Institute of Technology, Department of Mechanics, KTH, Stockholm.

Jiang, Y. (2015). *Free form finding of grid shell structures.* Thesis, University of Illinois at Urbana-Champaign, Civil & Environmental Engineering.

Konstantatou, M. (2019). *Geometry-based structural analysis and design via discrete stress functions.* PhD Dissertation, University of Cambridge, Department of Engineering.

L'Oceanografic, a. t. (2021). Retrieved from https://en.wikipedia.org/wiki/F%C3%A9lix_Candela#/media/File:L%27Oceanografic_(Valencia,_Spain)_01.jpg

Malek, S. (2012). *The effect of geometry and topology on the mechanics of grid shells.* Dept. of Civil and Environmental Engineering. Massachusetts Institute of Technology.

Maxwell, J. (1864). On Reciprocal Figures and Diagrams of Forces. *Philosophical Magazine and Journal of Science*, 26:250–261.

Maxwell, J. (1870). On Reciprocal Figures, Frames, and Diagrams of Forces. *Earth and Environmental Science Transactions of The Royal Society of Edinburgh, 26*(1), 1-40.

McRobie, A., Baker, W., Mitchell, T., & Konstantatou, M. (2016). Mechanisms and states of self-stress of planar trusses using graphic statics, part II: Applications and extensions. *International Journal of Space Structures, 31*(2-4), 102-111.

Miki, M., & Kawaguchi, K. (2010). Extended Force Density Method for form-finding of tension structures. *Journal of the International Association for Shell and Spatial Structures, 51*(4).

Miki, M., Adiels, E., Baker, W., Mitchell, T., Sehlström, A., & Williams, J. (2020). Form-finding of shells containing both tension and compression using the Airy stress function. *Preprints 2020, 2020120355*(December), 1-16. doi:10.20944/PREPRINTS202012.0355.V1

Mitchell, T., Baker, W., McRobie, A., & Mazurek, A. (2016). Mechanisms and states of self-stress of planar trusses using graphic statics, part I: The fundamental theorem of linear algebra and the Airy stress function. *International Journal of Space Structures, 31*(2-4), 85-101.

Olsson, J. (2012). *Form finding and size optimization-Implementation of beam elements and size optimization in real time form finding using dynamic relaxation.* Thesis, Chalmers University of Technology, Applied Mechanics, Gothenburg, Sweded.

Schek, H. (1974). The force density method for form finding and computation of general networks. *Computer Methods in Applied Mechanics and Engineering, 3*(1), 115-134.

Southern, R. (2011). *The force density method: A brief introduction.* Bournemouth: Bournemouth University.

Veenendaal, D., & Block, P. (2012). An overview and comparison of structural form finding methods for general networks. *International Journal of Solids and Structures, 49*(26), 3741-3753.

Williams, C., & McRobie, A. (2016). Graphic statics using discontinuous Airy stress functions:. *International Journal of Space Structures*(2-4), 121-134.

ANNEX I

Force Density Method Formulation in Python using gh PythonRemote

```
##### Import libraries
import ghpythonremote
import scriptcontext as sc
from ghpythonlib.treehelpers import list_to_tree
ssa = sc.sticky['scipy.sparse']
sci = sc.sticky['scipy']
np =sc.sticky['numpy']

lines = np.array(x)
lines = np.around(lines,decimals =4)
no_lines = len(lines)  # no_lines means no. of lines

##########get unique sets of points save them in matrix u and get indices in indices
lines = np.reshape(lines,(no_lines*2,2))
u,indices = np.unique(lines,return_inverse = True,axis = 0)
unqpt= np.unique(indices,return_inverse = False)
u_pt_len = len(indices)

############## CREATE CONNNECTIVITY MATRIX.
row = np.repeat(np.arange(no_lines),repeats =2 )
col = indices
data = np.tile([1,-1],no_lines)
cols = len(u)
C = ssa.csc_matrix( (data,(row,col)), shape = (no_lines,cols) ).todense()
CON = C.copy()

##############GET FIXED POINT INDEX FROM LIST OF UNIQUE POINTS
fxpt = np.array(fxpt)
fxpt = np.around(fxpt,decimals =4)
fxpt_id = np.lexsort((fxpt[:,1],fxpt[:,0]))
fxpt = fxpt[fxpt_id]
res = (u[:, None] == fxpt).all(-1).any(-1)
fxpt_indx = np.where(res)
rpt_indx = np.where(np.invert(res))


#############create Q and Qf matrix for fixed point and free point - connectivity matrices.
Qf = C[:,fxpt_indx]
Cf = np.reshape(Qf,(Qf.shape[0],Qf.shape[2]))
Qr = C[:,rpt_indx]
Cr = np.reshape(Qr,(Qr.shape[0],Qr.shape[2]))

##########CREATE DIAGONAL FORCE DENSITY MATRIX
q=np.array(q)
q = np.around(q,decimals =4)
Q=np.diag(q)


#################CREATE POINT LOAD VECTORS
p_x = np.zeros((len(u)-len(fxpt),1))
p_y = np.zeros((len(u)-len(fxpt),1))
p_z = np.tile(load,len(u)-len(fxpt))
p_z = np.reshape(p_z,(p_z.shape[0],1))

##########CREATE FIXED POINT CO-ORDINATE VECTORS
x_f = fxpt[:,0]
x_f = np.reshape(x_f,(x_f.shape[0],))
y_f = fxpt[:,1]
y_f = np.reshape(y_f,(y_f.shape[0],))
z_f=  np.full((x_f.shape[0],), 0)
```

```
###########CREATE D AND D_F
D = Cr.T.dot(Q).dot(Cr)
D_f = Cr.T.dot(Q).dot(Cf)

#GET THE CO-ORDINATES
x_ound = np.linalg.inv(D).dot(p_x - np.reshape(D_f.dot(x_f),(D_f.dot(x_f).shape[1],1)))
y_ound = np.linalg.inv(D).dot(p_y - np.reshape(D_f.dot(y_f),(D_f.dot(y_f).shape[1],1)))
z_found = np.linalg.inv(D).dot(p_z - np.reshape(D_f.dot(z_f),(D_f.dot(z_f).shape[1],1)))


############## EXPORT TO GRASSHOPPER FROM NUMPY ARRAY.
xx = np.ndarray.flatten(np.array(x_found))
xx = ghpythonremote.obtain(xx.tolist())
xx =list_to_tree(xx,source=[0,])

yy = np.ndarray.flatten(np.array(y_found))
yy = ghpythonremote.obtain(yy.tolist())
yy =list_to_tree(yy,source=[0,])

zz = np.ndarray.flatten(np.array(z_found))
zz = ghpythonremote.obtain(zz.tolist())
zz =list_to_tree(zz,source=[0,])


xxx = np.ndarray.flatten(np.array(x_ound))
xxx = ghpythonremote.obtain(xxx.tolist())
xxx =list_to_tree(xxx,source=[0,])

yyy = np.ndarray.flatten(np.array(y_ound))
yyy = ghpythonremote.obtain(yyy.tolist())
yyy =list_to_tree(yyy,source=[0,])
```

Mesh construction as per obtained points.

```
##### Import libraries
import rhinoscriptsyntax as rs
import ghpythonremote
import scriptcontext as sc
from ghpythonlib.treehelpers import list_to_tree
ssa = sc.sticky['scipy.sparse']
sci = sc.sticky['scipy']
np =sc.sticky['numpy']

########Convert arrays to numpy arrays
xx =np.array(x)
x=np.reshape(x,(len(x),1))
y = np.array(y)
y=np.reshape(y,(len(y),1))
z = np.array(z)
z = np.around(z,decimals=4)
z=np.reshape(z,(len(z),1))

###########Combine fix and free points
xedo = np.zeros((len(fxpt),1))
fxpt = np.hstack((fxpt,xedo))
fxpt_id = np.lexsort((fxpt[:,1],fxpt[:,0]))
fxpt = fxpt[fxpt_id]
xyz=np.concatenate((x,y,z),axis=1)

pt_num = len(fxpt)+len(x)
allpt = np.zeros((pt_num,3))
allpt[fxpt_indx] = fxpt
allpt[rpt_indx]=xyz

xedo = np.zeros((len(u),1))
u = np.hstack((u,xedo))
```

```
con =CON.copy()
cone =CON.copy()

con[con==1] =0
con[con==-1] = 1
spt = np.dot(con,allpt)

cone[cone==-1] =0
ept = np.dot(cone,allpt)

#PUSH DATA TO GRASSHOPPER TREE
sptx = ghpythonremote.obtain(spt[0:,0].tolist())
sptx =list_to_tree(sptx,source=[0,])

spty = ghpythonremote.obtain(spt[0:,1].tolist())
spty =list_to_tree(spty,source=[0,])

sptz = ghpythonremote.obtain(spt[0:,2].tolist())
sptz =list_to_tree(sptz,source=[0,])

eptx = ghpythonremote.obtain(ept[0:,0].tolist())
eptx =list_to_tree(eptx,source=[0,])

epty = ghpythonremote.obtain(ept[0:,1].tolist())
epty =list_to_tree(epty,source=[0,])

eptz = ghpythonremote.obtain(ept[0:,2].tolist())
eptz =list_to_tree(eptz,source=[0,])
```

ANNEX II

LATERAL LOADING IN VARIOUS SHELL GEOMETRIES

The comparison of effect of lateral loading (uniform static wind load) in deflection and total mass of the structure required to resist lateral and wind loading for various shell geometries are shown in Table 12.

Wind load intensity taken = 2 KNm^{-2}

Gravity loading = 5 KNm^{-2}

Grid shell Plan Dimensions = 12 m * 12m with 20 subdivisions in each side.

Grid shell Height taken = 3.5m

Table 11 Deflection and mass comparison table for lateral load in grid shells.

Grid shell type	Max deflection (mm)			Mass (kg)
	x	y	Z	
Spherical	2	0.4	1.5	1720.87
Pyramid	74	11.7	11.4	2608.08
Form found using FDM	1	0.4	0.8	1565.6

Table 12 Lateral load effects on various grid shell geometries

Shell and Loading type	Deflected Shape
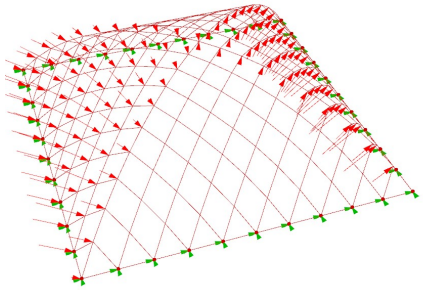 Figure 40 Grid shell geometry formed lofting edges to circular arc	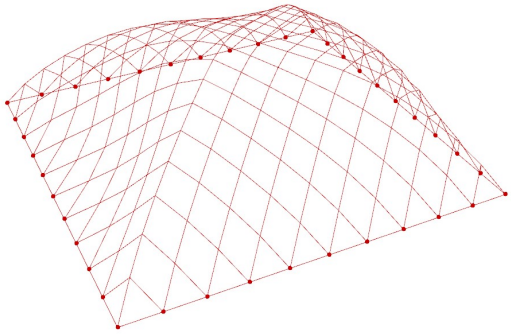
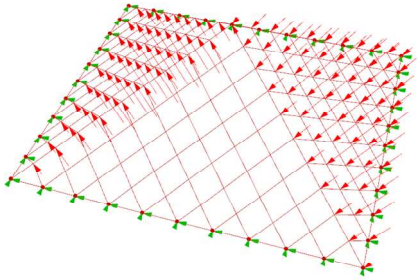 Figure 41 Grid shell constructed with pyramidal geometry	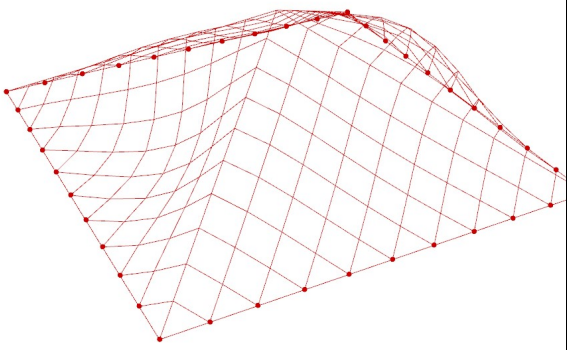
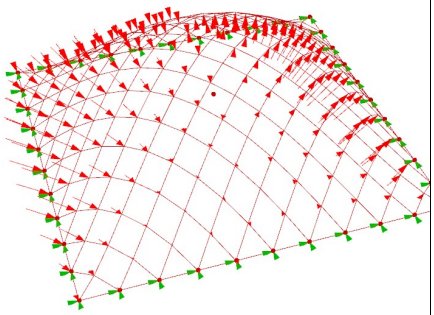 Figure 42 Form found grid shell